Gondwana Research 141 (2025) 213–227

Contents lists available at ScienceDirect

Gondwana Research

journal homepage: www.elsevier.com/locate/gr

Tectonic evolution of the Proto-Paleo-Tethys in the West Kunlun orogenic belt: Constraints from U-Pb geochronology of detrital zircons

Yang Gao [a,b,c,d], Lin Jiang [a,c,d,*], Weiyan Chen [c,d], Hongkui Dong [c], Fujie Jiang [a,b], Wen Zhao [c], Yingqi Feng [e], Liu Cao [a,b], Xuanwei Liu [a,b]

[a] National Key Laboratory of Petroleum Resources and Engineering, China University of Petroleum (Beijing), Beijing 102249, PR China
[b] College of Geosciences, China University of Petroleum (Beijing), Beijing 102249, PR China
[c] Research Institute of Petroleum Exploration and Development, PetroChina Beijing 10083, PR China
[d] CNPC Key Laboratory of Basin Structure and Hydrocarbon Accumulation, Beijing 10083, PR China
[e] School of Geosciences, China University of Petroleum (East China), Qingdao 266580, PR China

ARTICLE INFO

Handling Editor: Sanghoon Kwon

Keywords:
West Kunlun orogen belt
Detrital zircon U-Pb geochronology
Proto-Tethys
Paleo-Tethys
Mountain building

ABSTRACT

The West Kunlun piedmont tectonic belt was formed by the collision and accretion of the West Kunlun orogenic belt and the Tarim Craton. Its sedimentary record captures the processes of basin-mountain interactions, making it an excellent region for studying the formation of orogenic belts and the evolutionary history of the Tethys Ocean. Despite extensive research on the geological evolution of the West Kunlun orogenic belt by previous scholars, there remains considerable uncertainty regarding the initiation and termination times of oceanic crust subduction to the eventual closure for both the Proto-Tethys Ocean and the Paleo-Tethys Ocean in this region, as well as the temporal continuity between these two processes. This study obtained 703 detrital zircons with concordant ages from 9 core samples of Devonian to Cretaceous sandstones from 5 wells in the West Kunlun piedmont tectonic belt. Additionally, published detrital zircon data from the surrounding areas of the West Kunlun orogenic belt were collected from other studies for comparative analysis. The results indicate that the provenance of the piedmont tectonic belt during the Permian and Cretaceous periods primarily originated from the adjacent South and North Kunlun terranes. In contrast, during the Jurassic period, the provenance shifted to the Tianshuihai terrane. We infer that this change in sediment source was related to the closure of the Paleo-Tethys Ocean in the Late Triassic. Synthesizing previous research on magmatic rocks in the West Kunlun region, we identified two discontinuous orogenic cycles within the West Kunlun orogenic belt, which span from the Proto-Tethys Ocean to the Paleo-Tethys Ocean: the 560 Ma-380 Ma Proto-Tethys orogenic cycle and the 340 Ma–190 Ma Paleo-Tethys orogenic cycle. There was a distinct hiatus between the two cycles, during which the subdued volcanic activity during a tectonically stable period resulted in a minimal zircon record.

1. Introduction

The Tethys Ocean was a long-lived ancient ocean situated between the Laurasian and Gondwanan continents that existed from approximately 550 Ma to 23 Ma (Yin and Harrison, 2000; Wu et al., 2020), and its remnants were preserved in various orogenic belts, including the West Kunlun, East Kunlun, Altyn, and Qilian (Zhang et al., 2015; Zhang et al. (2004); Dong et al., 2021; Feng et al., 2023; Xiong et al., 2023). On the basis of its tectonic evolutionary history, the Tethys Ocean can be divided into three major oceans: Proto-Tethys, Paleo-Tethys, and Neo-Tethys. The tectonic evolution of the Neo-Tethys Ocean was marked by the collision and continued convergence between the Indian and Eurasian Plates, leading to the rapid uplift of the Tibetan Plateau during the Cenozoic Era (Huang et al., 2020; Zhang et al. (2004); Zhu et al., 2022). The continuous ocean-continent transitions and accretion-collision processes that occurred during the evolution of the Proto-Tethys and Paleo-Tethys Oceans resulted in the formation of a series of orogenic belts and fault zones, such as the West Kunlun orogenic belt, East Kunlun orogenic belt, Qilian orogenic belt, Altyn fault zone, and Karakoram fault zone, which collectively established the tectonic framework of the Tibetan Plateau. Therefore, understanding the ocean-continent configurations during different periods of the tectonic

* Corresponding author at: National Key Laboratory of Petroleum Resources and Engineering, China University of Petroleum (Beijing), Beijing 102249, PR China.
E-mail address: jianglin01@petrochina.com.cn (L. Jiang).

https://doi.org/10.1016/j.gr.2025.02.010
Received 3 May 2024; Received in revised form 18 January 2025; Accepted 24 February 2025
Available online 28 February 2025

evolution of the Proto-Tethys and Paleo-Tethys Oceans is crucial for deciphering the tectonic history of the plateau. Overall, the creation of the Proto-Tethys Ocean was related to the breakup of Rodinia during the Neoproterozoic (750 Ma-600 Ma) (Torsvik et al., 1998). The opening of the Paleozoic Tethys Ocean was triggered by the rollback of the Proto-Tethys Ocean slab (Reymond and Stampfli, 1996); however, the precise timing of the initiation of subduction to the complete the demise of the Proto-Tethys and Paleo-Tethys Oceans remains unclear, and it is also uncertain whether there was temporal continuity between them. Moreover, the northern Tibetan Plateau was formed by the assembly of multiple terranes from the Paleozoic to the Mesozoic, early scholars conducted relatively limited research on these Precambrian basement terranes (e.g., Tianshuihai, Qiangtang, and Songpan-Ganzi), they did not establish a comprehensive magmatic age distribution (Meert, 2003; Metcalfe, 2009). In recent years, although some scholars have begun conducting geochronological studies on these terranes to reconstruct the regional tectonic evolution of the Tethys Ocean, such efforts have generally been limited to individual terranes (Feng et al., 2023; Zhang et al., 2024). In fact, systematically studying these terranes that have experienced multiple tectonic and magmatic events could provide compelling insights into the tectonic evolution of the Proto-Tethys and Paleo-Tethys, as well as the formation of the northern orogenic belts (Li et al., 2018).

The spatiotemporal relationship between the Tethys Ocean and regional orogenic events is fundamentally a geological process driven by plate tectonics and the interactions among oceanic and continental plates (Deway and Horsfield, 1970; Li et al., 2016; Wan et al., 2019; Wu et al., 2020; Xiao et al., 2023). The opening, expansion, contraction, and eventual closure of the Tethys Ocean directly led to significant orogenic activity in the surrounding regions. The West Kunlun orogenic belt lies in the northern Tibetan Plateau and within the Central orogenic belt of China (Dewey et al., 1988). Its geological tectonic evolution involves not only the amalgamation and break-up of microcontinents but also the collision of island arcs, the continuous subduction of oceanic plates, the intrusion of basic and ultrabasic magmas and uplift of the orogenic belt (Zhao et al., 2018). It represents the product of the subduction of the Paleo-Tethys and Proto-Tethys Oceans and the accretion of continental and oceanic fragments from the early Paleozoic to the early Mesozoic (Zhang et al., 2008; Zhang et al., 2017). Therefore, the West Kunlun orogenic belt is considered a pivotal area for studying the formation and uplift of the Tibetan Plateau, as well as an important window for understanding the evolution of the Tethys Ocean (Mattern et al.,1996; Wang et al.,2004; Liu et al.,2019; Yin et al.,2020). Understanding the cyclical tectonic evolution of the Tethys Ocean and the formation of orogenic belts requires long-term records of tectonic events. In recent years, scholars have conducted a series of geochronological studies on major geological units such as igneous rocks and ophiolites along the Xinjiang-Tibet Highway and the China-Pakistan Highway to clarify the tectonic evolution of the West Kunlun region (Xu et al.,1994; Zhang et al.,1996; Gehrels et al.,2011; Mattern and Schneider.,2000; Mahar et al.,2016). However, because granites are extensively developed during various stages of orogenic cycles, including continental rifting, oceanic crust subduction, and continental collision, and owing to the complex nature of granites themselves, there are multiple interpretations regarding their genesis. For example, the timing of the closure of Proto-Tethys Ocean has been variously interpreted as occurring in the Ordovician, Silurian, or Devonian periods (Matte et al., 1996; Mattern and Schneider.,2000). The timing of the continental collision orogeny during the Paleo-Tethys cycle is subject to various interpretations, with some scholars proposing that it occurred in the Permian, others in the Triassic, and still others in the Jurassic (Zhang et al., 2005; Mo et al., 2006; Yang et al., 2010). To date, the tectonic evolution of the Proto-Tethys and Paleo-Tethys in the West Kunlun region remains a subject of debate (Pan, 1996; Jiang et al., 2002; Yang et al., 2007; Mahar et al.,2014; Zhang et al., 2018).

As one of the most stable minerals in sediments, detrital zircons can provide critical information for tracing sedimentary provenances and ages. In recent years, zircons have been widely used in studies on the formation and evolution of plates and orogenic belts (Schwab et al.,2004; Eizenhöfer et al., 2014, 2015, Eizenhöfer and Zhao (2018); Wang et al.,2020;Wu et al.,2020;Zhu et al.,2021; Li et al., 2024). Sedimentary strata buried several kilometres underground record the changes in lithological sequences from the basement to the surface. Compared with igneous rocks with single intrusions, sedimentary rocks provide a more comprehensive record of regional sedimentary conditions and offer more effective constraints for understanding long-term geological evolution. This paper presents a U-Pb geochronological study of the detrital zircons obtained from Devonian to Cretaceous sedimentary rocks located in the West Kunlun piedmont tectonic belt, providing a detailed provenance analysis for each stratigraphic level. By integrating previous research, this paper proposes the latest perspectives on the tectonic evolution of the Proto-Tethys and Paleo-Tethys in the West Kunlun orogenic belt and further explores the formation and uplift processes of the West Kunlun orogenic belt.

2. Geological setting

The West Kunlun orogenic belt (WKOB) is located in the northwestern part of the Tibetan Plateau and is bounded by the Tarim Basin to the north, the Qiangtang terrane to the south, the Pamir Plateau to the west, and the Altun fault zone to the east (Fig. 1. A). There are three main fault zones in its interior, namely, the Kudi suture, Kangxiwar suture and Hongshanhu suture, from north to south. Bounded by these fault zones, the orogenic belt can be divided into three terranes from north to south, namely, the North Kunlun terrane (NKT), the South Kunlun terrane (SKT) and the Tianshuihai terrane (TSHT) (Fig. 1. B) (Pan and Bian, 1996; Xiao et al., 1999). The West Kunlun orogenic belt has undergone a complex tectonic evolutionary process associated with the Proto-Tethys and Paleo-Tethys oceans, accompanied by frequent magmatic activity.

The North Kunlun terrane (NKT) is believed to be the uplifted southwestern margin of the Tarim Craton and a part of the Tarim Plate (Zhang et al. (2018b), Zhang et al. (2016)). The Precambrian metamorphic basement is well exposed in this area and includes the Paleoproterozoic Heluositan complex, the Mesoproterozoic greenschist-to amphibolite-facies metamorphosed and intensely folded sedimentary sequences (the Kalakashi Group), the mid-Neoproterozoic greenschist-facies metamorphism and folded volcano-sedimentary sequences, and the late Neoproterozoic unmetamorphic carbonate-clastic-tillite sequences (Zhang et al., 2019). The sedimentary cover consists of Devonian molasse, Carboniferous-Permian shallow marine carbonate rocks and late Permian continental sedimentary rocks. The magmatic records found within the terrane are relatively sparse, with ages ranging primarily from 510 Ma to 460 Ma (Cui et al., 2007; Chen et al., 2020). Previous studies have interpreted these records as products of the subduction process of the Proto-Tethys Ocean.

The South Kunlun terrane (SKT) is considered an exotic block that moved to the southern margin of the Tarim Plate during the late Neoproterozoic to the early Paleozoic (Yuan et al., 2002; Xiao et al. (2003a)). Like the NKT, the Precambrian basement is exposed in this terrane, which includes Paleoproterozoic gneisses, migmatites, amphibolites and schists, and Mesoproterozoic schists, gneisses, marbles and amphibolites (Jia et al., 2013). The sedimentary cover primarily consists of siliciclastic rocks, carbonates and calc-alkaline volcanic rocks from the early Paleozoic to the Mesozoic (Pan and Wang, 1994; Yuan et al., 2002). Previous studies have identified a substantial number of Mesozoic to Paleozoic magmatic rock records in this block, with ages ranging from 520 Ma to 190 Ma. These records correspond to the evolutionary timeline of the Proto-Tethys Ocean to the Paleo-Tethys Ocean (Kang et al., 2015; Sui et al., 2021; Allen et al., 2023). A series of early Paleozoic to early Mesozoic intrusive rocks have been found in the Precambrian basement (Jiang et al., 2013; Liu et al., 2015), which

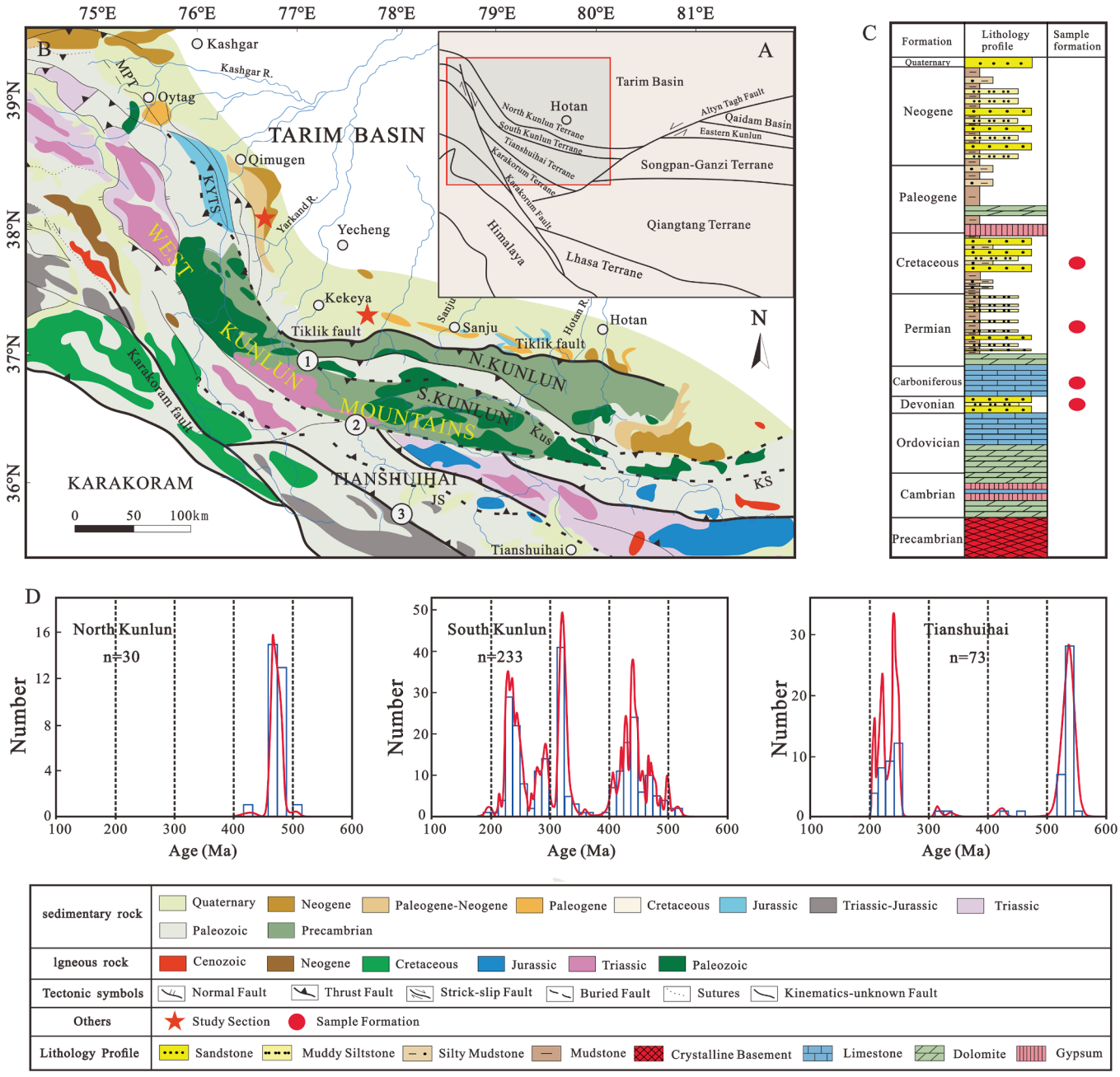

Fig. 1. (A) the sketch map showing the location of the study area. (B) Geological map of the Pamir, West Kunlun Mountain, SW Tarim Basin and adjacent areas (modified after Cao et al., 2015; Yang et al., 2018). (1) Kudi suture; (2) Kangxiwar suture. (3) Hongshanhu suture. MPT, Main Pamir Thrust; Kus, Kudi suture; KS, Kongur Shan; KYTS, Kashgar-Yecheng Transfer System; JS, Jinsha Suture. (C) Lithologic column map and label of sampling horizon in West Kunlun piedmont tectonic zone. (D) The distribution of magmatic rock ages across different terranes within the West Kunlun orogenic belt.

corresponds to magmatism in the NKT, indicating that the two may have collided in the early Paleozoic.

Owing to its remote geographical location and coverage by large glaciers, the Tianshuihai terrane (TSHT) has been the subject of considerable controversy in recent years regarding its tectonic nature. Some scholars have proposed that the TSHT is related to the late Paleozoic to early Mesozoic orogenic process of a large accretionary prism (Xiao et al., 2005), and some scholars believe that the TSHT is an independent continental block with a Precambrian basement and that its lithology is dominated by green schist, granulite and marble (Qiao et al., 2015; Hu et al., 2016). Previous studies in this terrane have identified two phases of magmatic records, the early Paleozoic and the early to middle Mesozoic (Gao et al., 2013; Zhu et al., 2016; Wei et al., 2018; Sui et al., 2021; Lu et al., 2022).

The West Kunlun piedmont tectonic belt (WKPB), located to the north of the NKT, is the transitional region between the West Kunlun orogenic belt and the Tarim Plate and is a part of the Tarim Basin (Jiang et al., 2024). The Precambrian basement is exposed in this area, and the lithology consists of metamorphic rocks and granite. The sedimentary cover includes limestone, sandy conglomerate and Paleozoic, Mesozoic and Cenozoic mudstones, while Triassic layers are missing (Fig. 1. C).

3. Sampling and methods

We collected 9 core samples from 5 wells (Kd5, Kd101, T1, Ky1 and S2) in the central and southern parts of the WKPB from the late Paleozoic

to late Mesozoic. They include four Cretaceous sandstones (Kd5-5138.0, Kd5-5143.5, Kd5-5790.4, and Kd101-2976.34); one Jurassic sandstone (Kd101-4316.3); one Permian sandstone (T1-4201.1); two Carboniferous sandstones (Ky1-4786.2 and Ky1-4789.8) and one Devonian sandstone (S2-5843.8). The depth of each well sample is indicated by the number following the well name in the sample identifier. For example, the depth of sample Kd5-5138.0 is 5138.0 m. The locations of the 5 wells are distributed in a concentrated manner, mainly in 2 areas (Study Section of Fig. 1. B).

Each sandstone sample underwent mechanical crushing, washing, magnetic separation, and heavy liquid separation before more than 200 zircon grains were selected under a binocular microscope and mounted them on double-sided tape. The grains were then embedded in epoxy resin to create targets, with each sample containing more than 150 zircon grains on average. Once the epoxy resin fully cured, the samples were polished to expose the zircon surfaces and internal structures. The polished sample targets were then photographed via transmitted/reflected light and cathodoluminescence (CL) imaging to determine the internal structures of the zircon grains, while avoiding fractures and inclusions during the analysis.

Zircon U–Pb dating was completed on a laser ablation inductively coupled plasma mass spectrometer (LA-AICP-MS) at the Key Laboratory of Basin Structure and Hydrocarbon Accumulation, Petroleum Geology Experimental Research Center, Research Institute of Petroleum Exploration and Development, China. An NWV 193 nm laser and an Element SF-ICP-MS mass spectrometer were used. Comparing the photographs of transmitted/reflected light as well as cathodoluminescence images, zircon grains without fractures or inclusions were selected for analysis, and the denudation positions were marked. The instrument signal was tuned using NIST614 to obtain the best test conditions, and the laser denudation parameters were determined, including a spot size of 30 μm and a denudation frequency of 3 Hz. In this study, 100 samples were randomly selected for analysis so that the analysis results could reflect the source characteristics. For the selected denudation sites, every eight denudation sites were interlaced with a set of standard samples for data corrections, including the international standard zircons NIST610, 91,500 and PLE. Iolite software was used for baseline corrections and blank deductions to form the final data. Finally, Isoplot 4.15 software was used to calculate the ages and generate the graph. If the zircon age $\geq$ 1000 Ma is $^{207}Pb/^{206}Pb$, the zircon age $\leq$ 1000 Ma is $^{206}Pb/^{238}U$. Using the ratios of $^{206}Pb/^{238}U$ and $^{207}Pb/^{235}U$ as a method to calculate concordance, the measured ages are considered concordant when the zircon age concordance falls between 1.1 and 0.9.

Owing to the characteristics of the mixed-age peaks in the detrital zircons obtained from sedimentary rocks, merely comparing the peak values introduces bias. Statistical methods can assist in inferring differences between samples and their similarities with other datasets from a data-driven perspective, thereby achieving more precise conclusions. This study employs the Kolmogorov-Smirnov nonparametric test (K-S test) method to conduct a comparative analysis of the correlations among the zircon U-Pb age data from various samples and potential source data. The K-S test is a statistical method that involves constructing cumulative probability distribution curves for zircon U-Pb age data from different datasets and then calculating the P value to assess the similarities and differences between the samples. When $P \leq 0.001$, there is a significant difference between the two sample age datasets; when $0.001 < P \leq 0.05$, the difference between the two datasets is not significant; when $P \geq 0.05$, there is no significant difference between the two datasets; that is, the two samples are highly likely to come from the same population. The K-S test has certain limitations, as it does not account for the inherent uncertainty or error associated with each zircon U-Pb age measurement. This lack of considering uncertainties may affect the accuracy of the analysis. However, the K-S test has the advantage of a relatively simple computational process, which is based on the maximum difference between two distribution functions. The results, particularly the D value (maximum difference) and the corresponding P value, are straightforward to interpret and can directly indicate whether there are significant differences between the distributions of two samples.

The changes in the Tethys Ocean are closely related to the formation of the WKPB. Detrital zircons from the piedmont tectonic belt are sourced primarily from various terranes within and near the basin and orogenic belt. To better assess the potential sources of detrital zircons in sedimentary deposits from the late Paleozoic to late Mesozoic in the piedmont tectonic zone, we compiled published zircon U-Pb age data from different formations in the Songpan-Ganzi (SPGZ), East Kunlun orogenic belt (EKOB), Qiangtang (QT), Tianshuihai terrane (TSHT), Qilian, Tarim, South and North Kunlun terranes (SNKL) and plotted them as cumulative curves and age spectra (Figs. 5 and 6). The mixed source data from the SNKL were derived from modern river sand samples from the Karakash River and the Tiznip River, both of which traverse the SNKL. The SPGZ provided zircons from the Triassic and Devonian, the EKOB provided zircons from the Triassic and Permian, the QT provided zircons from the Triassic and Carboniferous, zircons from the Qilian Orogen were metamorphic, and the TSHT provided zircons from the Cambrian and Triassic. Notably, these surveyed terranes exhibit complex age distributions with multiple peaks, indicating their involvement in intricate tectonic and evolutionary cycles prior to their assembly. These processes were closely related to the formation and fragmentation of Gondwana, Rodinia, and the amalgamation movements of Gondwana.

4. Results

4.1. Morphology and geochronology of detrital zircon

In this study, a total of 900 detrital zircon grains from 9 samples were selected for U-Pb isotope age testing, 703 of which yielded concordant ages. We observed the morphological characteristics of each sample and randomly selected 6 zircon grains from the age range of each sample to create images (in the supplementary materials). We conducted a preliminary grouping of the zircon ages in the study samples on the basis of the distribution of magmatic rocks in the West Kunlun orogenic belt depicted in Fig. 1D, using 200 Ma, 400 Ma, and 600 Ma as demarcation points; the U-Pb concordia diagram is shown in Fig. 2; and the age distribution histogram and relative probability diagram are shown in Fig. 3. We identified age peaks on the basis of Fig. 3; these peaks are approximations and have not been rigorously calculated.

4.1.1. Devonian samples

A total of 100 zircons were analysed from the Devonian sample S2-5843.8, all of which are of concordant age. The majority of the zircon grains in this sample are intact, with only a small number being fragmented. The zircon grains are predominantly subhedral and have good roundness in shape, with grain sizes ranging between 50 μm and 140 μm and length-to-width ratios ranging from approximately 1:1 to 3:1. The maximum age of the zircon grains in this sample is 2739 ± 104 Ma, and the youngest is 412 ± 15 Ma. The U-Pb ages can be roughly divided into 501 Ma-412 Ma (with a peak age of 436 Ma) and 2739 Ma-631 Ma (with two peak ages of 1695 Ma and 801 Ma). The two age groups accounted for approximately 28 % and 72 %, respectively.

4.1.2. Carboniferous samples

The two carboniferous samples are Ky1-4789.8 and Ky1-4786.2. In both samples, the majority of zircons exhibit intact morphologies, with only a few showing fragmentation. The zircon grains are predominantly subhedral and exhibit good roundness. The grains are relatively large, with sizes ranging from 100 to 250 μ m and length-to-width ratios ranging from approximately 1:1 to 4:1. Sample Ky1-4789.8 yielded 98 concordant zircon ages. Excluding the ages of 596 Ma and 593 Ma, all other zircon ages are above 600 Ma. The maximum age of a single zircon grain is 3017 ± 79 Ma. Kernel density estimation reveals three major

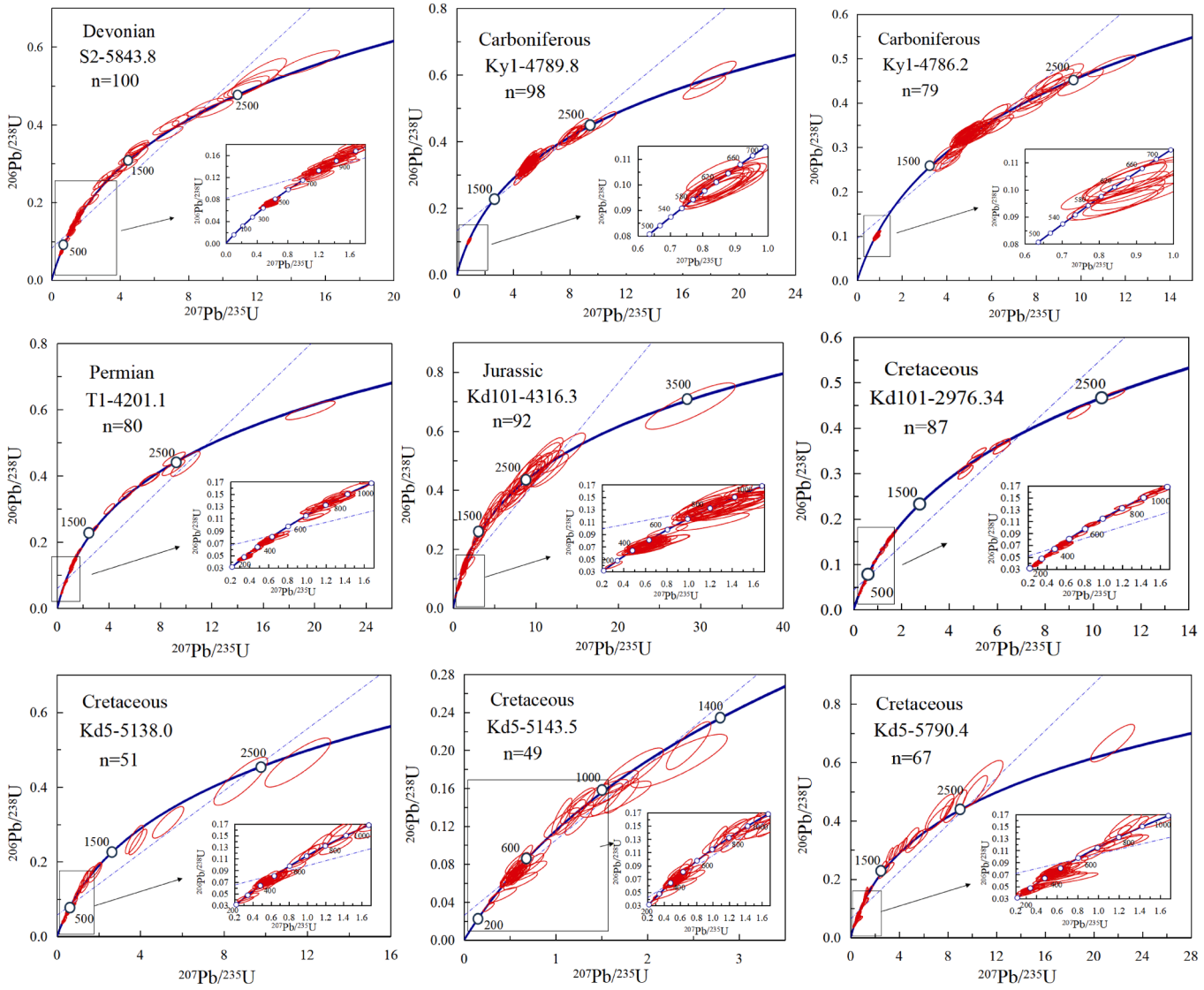

Fig. 2. U-Pb Concordia plots for detrital zircon U-Pb ages of the nine analyzed samples in the West Kunlun piedmont tectonic belt.

peaks at 2267 Ma, 1801 Ma, and 611 Ma. Sample Ky1-4786.2 yielded 79 concordant zircon ages. Four zircons exhibited ages younger than 600 Ma: 598 Ma, 591 Ma, 589 Ma, and 580 Ma. All other zircon ages are greater than 600 Ma, with the maximum age of a single zircon grain being 2518 ± 79 Ma. The probability density estimation reveals three major peaks at 2255 Ma, 1752 Ma, and 620 Ma.

4.1.3. Permian samples

The 100 ages analysed from the Permian t1-4201.1 sample yield 80 concordant ages. The majority of zircon grains in this sample are intact, with a small number showing signs of fragmentation. The zircon grains are predominantly long and prismatic in shape, with sizes ranging between 50 and 130 μ m and length-to-width ratios ranging from approximately 1:1 to 5:1. In this sample, the maximum zircon age is 3073 ± 103 Ma, and the youngest age is 274 ± 10 Ma. The U-Pb age distribution can be roughly divided into three intervals: 390 Ma-274 Ma, 523 Ma-433 Ma, and 3073 Ma-680 Ma. The probability density estimation reveals three major peaks at 867 Ma, 448 Ma, and 290 Ma. Additionally, zircons in the age range of 390 Ma-274 Ma constitute the majority, accounting for approximately 42.5 % of the sample.

4.1.4. Jurassic samples

For the Jurassic sample Kd101-4316.3, a total of 100 zircons are analysed, 8 of which exhibit discordant ages. In this sample, the majority of zircons exhibit intact morphologies, with a small number showing signs of fragmentation. The zircon grains are predominantly euhedral, and mostly angular in shape, with sizes ranging from 80 to 250 μ m and length-to-width ratios ranging from approximately 1:1 to 5:1. The maximum age of the zircon grains in this sample is 3320 ± 132 Ma, and the youngest is 255 ± 29 Ma. Two zircons exhibit U-Pb ages younger than 400 Ma, specifically 399 Ma and 255 Ma. The remaining zircon ages can be roughly divided into two groups: 584 Ma-409 Ma and 3320 Ma-669 Ma. The proportions of zircons in these two age ranges are approximately 30.4 % and 67.4 %, respectively. The probability density estimation reveals three major peaks at 2260 Ma, 802 Ma, and 444 Ma.

4.1.5. Cretaceous samples

There are four Cretaceous samples, namely, Kd5-5138.0, Kd5-5143.5, Kd5-5790.4 and Kd101-2976.34. Among the four samples, the majority of the zircon grains are intact, with only a small number showing fragmentation. The zircon grains are predominantly euhedral and angular in shape, with sizes ranging from 60 to 250 μ m and length-to-width ratios ranging from approximately 1:1 to 4:1.

For sample kd5-5138.0, a total of 100 zircons are analysed, with 51 yielding concordant ages. These ages can be roughly divided into three intervals: 385 Ma-247 Ma, 565 Ma-407 Ma, and 2606 Ma-674 Ma. The

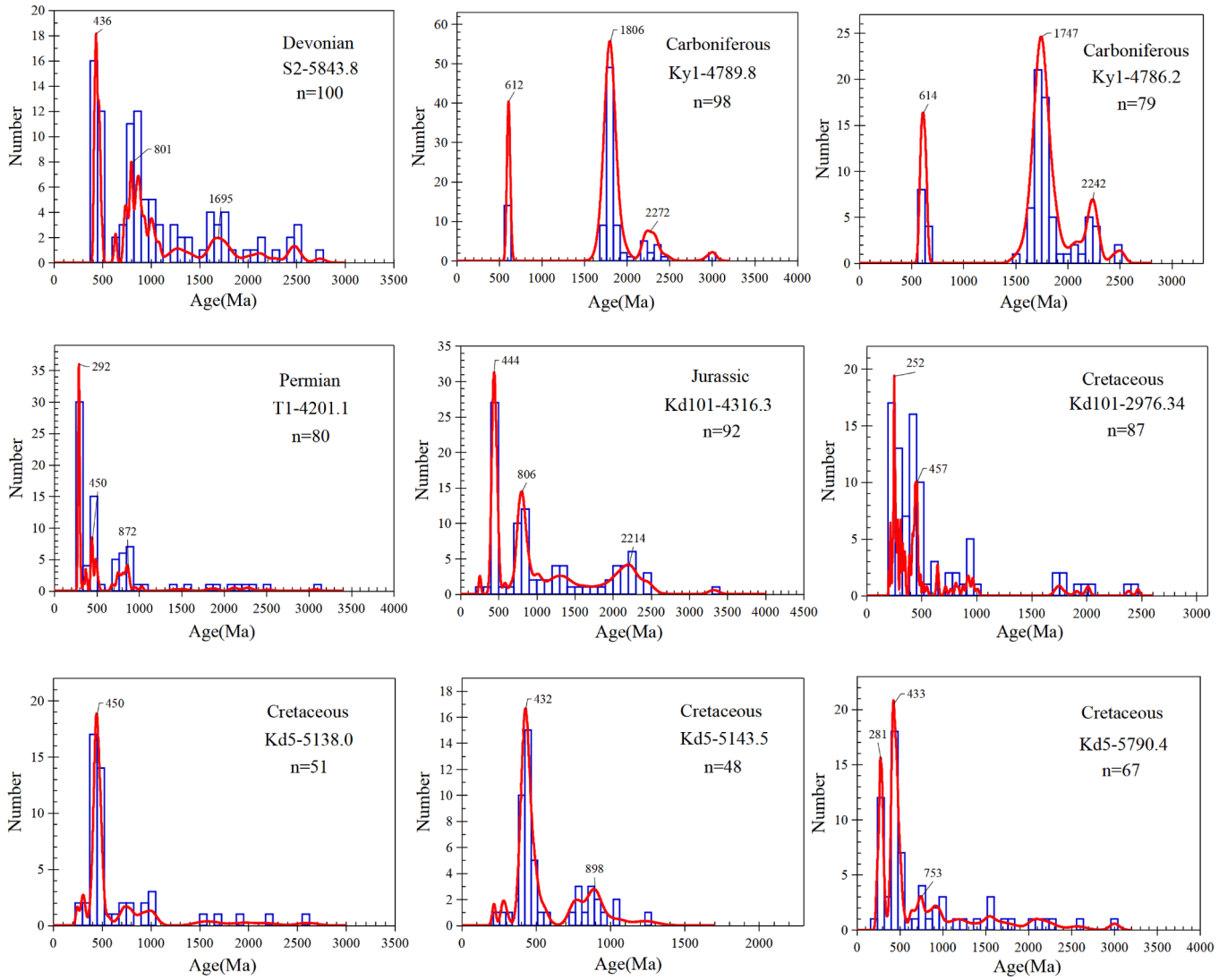

Fig. 3. Histograms and normalized probability curves of ages of detrital zircons from sedimentary samples of the West Kunlun piedmont tectonic belt.

probability density estimation analysis identified the most prominent age peak at 451 Ma. Zircons in the 565 Ma-407 Ma age range constitute the majority, accounting for approximately 60.7 % of the sample.

From the well Kd5 sample Kd5-5143.5, a total of 100 zircons are analysed, with 49 yielding concordant ages. The maximum zircon age in this sample is 1237 ± 145 Ma, and the youngest age is 218 ± 23 Ma. The U-Pb age distribution can be roughly divided into three intervals: 389 Ma-218 Ma, 562 Ma-407 Ma (with a peak at 436 Ma), and 1237 Ma-746 Ma (with a peak at 911 Ma). These three age groups account for 10.2 %, 61.2 %, and 28.6 % of the sample, respectively.

From well Kd5 sample Kd5-5790.4, a total of 100 zircons are analysed, with 67 yielding concordant ages. The maximum zircon age in this sample is 3001 ± 107 Ma, and the youngest age is 232 ± 22 Ma. The U-Pb age distribution can be roughly divided into three intervals: 396 Ma-232 Ma (with a peak at 278 Ma), 548 Ma-411 Ma (with a peak at 430 Ma), and 3001 Ma-634 Ma (with a peak at 764 Ma). The proportions of zircons in these three age ranges are approximately 23.9 %, 37.3 %, and 38.8 %, respectively.

A total of 100 zircons are analysed in the kd101 well sample Kd101-2976.34, with 87 yielding concordant ages. The maximum zircon age is 2469 ± 30 Ma, and the youngest age is 204 ± 7 Ma. The U-Pb age distribution can be roughly divided into three intervals: 399 Ma-204 Ma (with a peak at 252 Ma), 548 Ma-414 Ma (with a peak at 460 Ma), and 2469 Ma-645 Ma (without a distinct peak). Zircons in the 399 Ma-204 Ma and 548 Ma-414 Ma age ranges constitute the majority, accounting for approximately 44.8 % and 28.7 % of the sample, respectively.

Cretaceous zircons generally exhibit discordant ages, which could be attributed to intense tectonic compression during the Cretaceous period. This compressional event generated extremely high temperatures and pressures, under which zircons may have undergone recrystallization or partial melting. These processes can lead to the redistribution of the uranium-lead (U-Pb) system, resulting in age determinations that deviate from the original formation ages of the zircons.

4.2. *The Th/U ratios of detrital zircons*

Overall, most zircon grains exhibit magmatic origins with oscillatory zoning, whereas some display uniform internal structures or weak oscillatory growth zoning. A very small number of zircon grains present thin, bright, and overgrown metamorphic zircon CL images. Among the 703 concordant zircon grains, 690 have Th/U ratios greater than 0.2, accounting for 98.15 % of the total, which provides substantial evidence to differentiate between magmatic zircons (Th/U > 0.2) and metamorphic zircons (Th/U < 0.1) (Fig. 4). The combined morphological and Th/U analyses suggest that our samples are predominantly of magmatic origin and that the U-Pb ages primarily represent zircon crystallization times.

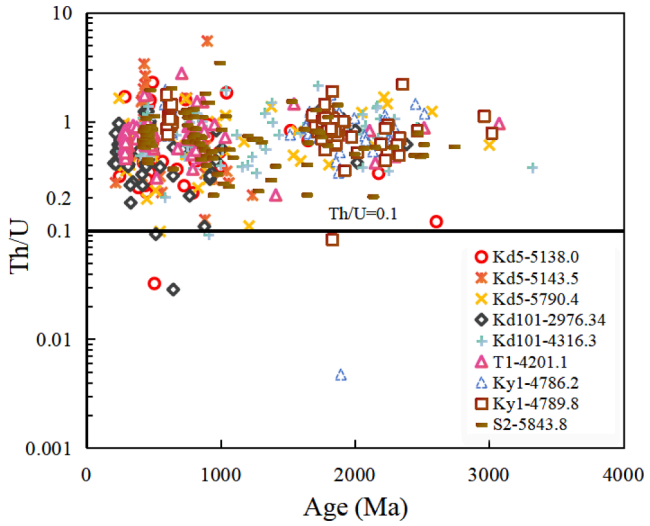

Fig. 4. Th/U vs. ages for zircons analyzed in this study.

4.3. Kolmogorov–Smirnov nonparametric test

In this K-S test, two understandings from a geological perspective were followed: first, the older strata in the piedmont tectonic belt cannot provide the source material for the younger strata of the orogenic belt; second, the younger strata cannot provide the source material for the older strata. In the probability density plot, the Carboniferous samples exhibit significant differences compared with the other samples, whereas the relationships among the other curves require further numerical representation for clarification. In the statistical results (in the supplementary materials), orange represents P values greater than 0.05, yellow indicates P values between 0.05 and 0.001, and blue signifies P values greater than 0.001 but do not conform to the aforementioned two principles. The results of the K-S test conducted on the datasets between samples indicate a significant correlation between the Cretaceous and Permian samples (with one P value of 0.081 and two P values greater than 0.001), suggesting that they are highly likely to originate from the same source region. The results of the K-S test conducted on the datasets between samples and potential source regions indicate the following: first, the four Cretaceous samples show no significant differences from the East Kunlun orogenic belt and the North and South Kunlun terranes (with a P value of 0.389 and three P values greater than 0.001). Additionally, one Cretaceous sample is not significantly different from the Triassic strata of the Tianshuihai terrane (with a P value of 0.031). Second, the Jurassic samples exhibit minimal differences from the Songpan-Ganzi Devonian samples (with a P value of 0.084) and show no significant differences from the East Kunlun Permian samples and Tianshuihai samples (with P values of 0.016 and 0.002, respectively). Third, the Permian samples demonstrate no significant differences from the North and South Kunlun terranes (with a P value of 0.031). Fourth, the two Carboniferous samples show no correlation with any of the datasets, which may indicate a mixed source similar to that of the Carboniferous samples from the Songpan-Ganzi, Tianshuihai, and Qiangtang regions. Fifth, the Devonian samples are significantly correlated with the Songpan-Ganzi Devonian samples (with a P value of 0.301). Sixth, although the Devonian samples show no significant differences from the East Kunlun Permian samples and Tianshuihai terrane samples(with P values both greater than 0.001), they violate the first principle of this K-S test and therefore should not be considered. Seventh, the Qiangtang block and Tianshuihai terrane exhibit no significant differences from the Songpan-Ganzi terrane (with P values greater than 0.001). Additionally, the Cambrian strata of the Tianshuihai terrane are not significantly different from the Carboniferous strata of the Qiangtang Block (with a P value of 0.005).

5. Discussion

5.1. Zircon sources and related regional tectonic thermal events

The zircon samples analysed in this experiment exhibit a wide age distribution, spanning multiple geological eras from the Archean to the Mesozoic. By correlating the zircon ages with the timing of regional tectonothermal events, we can further elucidate their provenance characteristics and the history of magmatic activity, providing crucial data for reconstructing the tectonic evolution of the region.

5.1.1. Archean to Neoproterozoic detrital zircons

The maximum age of the 9 samples from the Cretaceous to the Devonian from the 5 wells in the WKPB is 3320 ± 132 Ma. All the Archean to Paleoproterozoic zircons can be divided into two groups according to their peak age distributions, which are 1600 Ma-1900 Ma and 2200 Ma-2600 Ma, respectively, and some of these zircons are older than 2600 Ma. An age of 3.14 Ga has been found for the granulite samples from the Tiklik area, NKT (Guo et al., 2013), indicating that there may be an Archean paleocontinental core basement in the Tarim Basin, which corresponds to the oldest zircon age of 3.32 Ga obtained in this experiment. However, zircons older than 3.0 Ga have been found in sediments from Australia, India and Antarctica (Cawood et al., 2000; Turner et al., 2014; Paulsen et al., 2016), and the possibility of zircons undergoing depositional cycles cannot be ruled out. A crustal accretion event occurred at approximately 2.5 Ga in many parts of the world, and magmatic records of this stage have been found in Tarim, South China, and West Africa. The zircons of this age in this study may be records of this accretion event (Zhao et al., 2009; Shu et al., 2011; Liu et al., 2017). There is a continuous zircon record between 2.5 Ga and 2.0 Ga, which

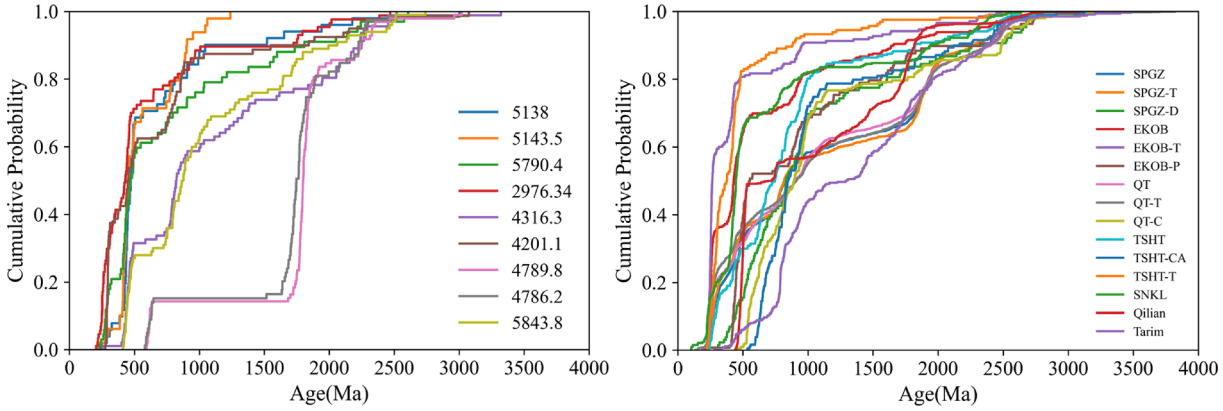

Fig. 5. Cumulative probability density plots for the sandstone samples used in this study.

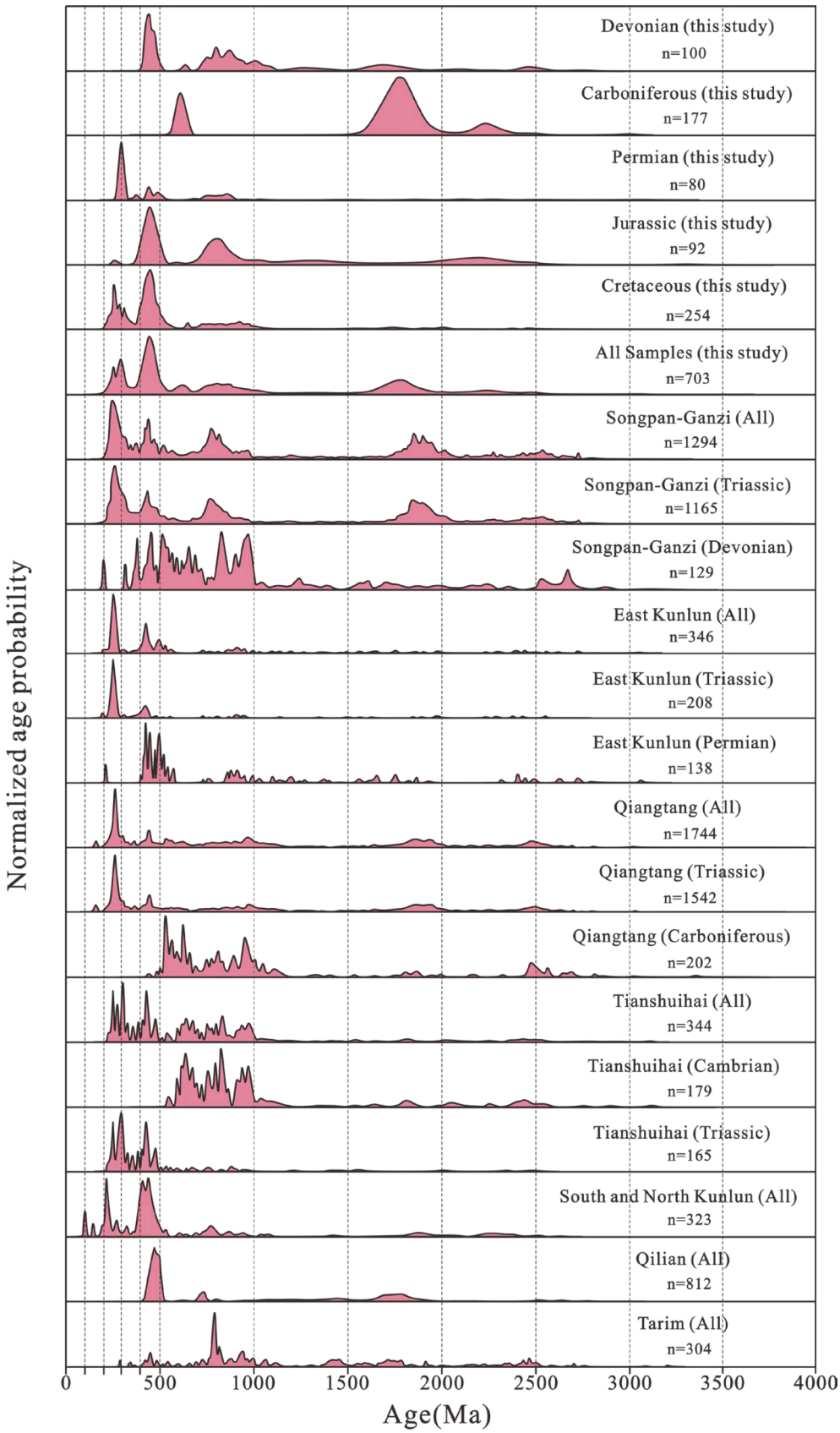

Fig. 6. Zircon U-Pb age and U-Pb age distribution of detrital zircon in potential provenance area of the West Kunlun Mountains. Songpan-Ganzi (Triassic) (Ding et al., 2013); Songpan-Ganzi (Devonian) (Liu, 2006); East Kunlun (Triassic) (Ding et al., 2013); East Kunlun (Permian) (Hu, 2014; Huang, 2016); Qiangtang (Triassic) (Ding et al., 2013; Gehrels et al., 2011); Qiangtang (Carboniferous) (Gehrels et al., 2011); Tianshuihai (Cambrian)(Hu et al., 2016); Tianshuihai (Cambrian) (Dong et al., 2019); South and North Kunlun (Blayney et al., 2016); Qilian (Xiong et al., 2023); Tarim (Rojas-Agramonte et al., 2011).

corresponds to the magmatic activity that occurred in the southwestern Tarim region during the early Paleoproterozoic. The evidence for this includes the Cambrian Huoerguosi granitic complex, whose ages range from 2.4 Ga to 2.32 Ga (Zhang et al. (2007a), Zhang et al. (2007b); Ye et al., 2016). A significant number of magmatic records from 2.0 Ga to 1.8 Ga have been found in the Tarim Craton and its surrounding regions (Ge et al., 2013; Zhang et al., 2014; Lu et al., 2008). These records correspond to the global collisional events of 2.1 Ga to 1.8 Ga during the Paleoproterozoic (Zhao et al., 2002; Santosh et al., 2006), indicating that the Tarim Craton and its surrounding regions were influenced by the assembly of the Columbia supercontinent and experienced significant collisional and orogenic events from 2.0 Ga to 1.7 Ga (Zhang et al., 2012; Zhu et al., 2021; Ge et al., 2022), aligning with the Paleoproterozoic zircon age peak of 1.8 Ga observed in this study.

During the Mesoproterozoic era, the Tarim block underwent extensive passive continental margin sedimentation, and there is little evidence of volcanic activity in the Tarim block during this period. The late Mesoproterozoic to early Neoproterozoic marked the formation time of the Rodinia supercontinent; however, previous studies have failed to identify zircon age peaks in the Tarim block (Zhou et al., 2021; Yi et al., 2023), this finding corresponds with the minimal presence of zircon ages ranging from 1.5 Ga to 0.9 Ga obtained in this study. Neoproterozoic (approximately 830 Ma-720 Ma) global-scale intraplate magmatic activity has been extensively recorded in Australia, South China, and Tarim, which is usually inferred to be related to the fragmentation of the Rodinia supercontinent caused by mantle plumes or superplumes (Park et al., 1995; Song et al., 2010; Peng et al., 2019). This magmatism has left large-scale rock records in the WKOB and adjacent areas, such as large-scale basic dike groups in the Aksu and WKOB and many igneous rock units (800 Ma-720 Ma) in the Altun and Qaidam blocks (Xu et al., 2016), which may have been the source for the 900 Ma-750 Ma detrital zircons. In addition, 700 Ma-600 Ma granites have been recorded in parts of the Tarim and Australia blocks and are presumed to be related to the convergence of the Gondwana supercontinent at the end of the Neoproterozoic (Ge et al., 2012; Kendall et al., 2006), which may have been the source of the 650 Ma-600 Ma detrital zircons.

5.1.2. Paleozoic and Mesozoic detrital zircons

Paleozoic and Mesozoic zircons are the most concentrated age groups of all detrital zircons. The Tianshuihai region has abundant exposures of magmatic rocks with ages ranging from 540 Ma to 510 Ma, a characteristic not observed in magmatic rocks from other terranes in the WKOB or adjacent Tethyan domains (Allen et al., 2023). We infer that the zircons with ages greater than 510 Ma in this study originated from the Tianshuihai terrane. Seven of the nine samples produced age peaks at 460 Ma-430 Ma, which are related to the active tectonics of the WKOB and its periphery beginning in the early Paleozoic. Many magmatic rocks from 500 Ma to 400 Ma have been discovered in both the NKT and the SKT. This is attributed to extensive subduction and consumption of the early Paleozoic Proto-Tethys Ocean, which led to the formation of a significant magmatic arc in the West Kunlun region during the early Paleozoic (Liu et al., 2014; Zhang et al., 2018a), and this subduction was accompanied by the closure of the Proto-Tethys Ocean on the southern side of the Tarim Basin (Yuan et al., 2002; Xiao et al., 2005; Liu et al., 2014). On this basis, the 500 Ma-400 Ma zircons are believed to have originated from intense magmatic activity. A small number of zircons aged 400 Ma-300 Ma are present in the samples. Previous studies have identified abundant 330 Ma to 310 Ma plagiogranites in the northwestern part of the SKT (Kang et al., 2015) and 338 Ma hornblende quartz diorites in the Kangxiwar tectonic mélange belt on the southern side of the SKT (Li et al., 2006). These granites have been interpreted as related to subduction processes in the ancient Tethys Ocean. We hypothesize that the zircons from this age range may originate from magmatic activities recorded in the SKT. Three of the nine samples recorded peaks in the 300 Ma to 250 Ma range (the remaining samples were not recorded because of the inconsistency of stratigraphic age and age discordant): Permian sample t1-4201.1 and two Cretaceous samples kd101-2976.34 and kd5-5790.4. These peaks correspond to subduction processes in the ancient Tethys Ocean. The widespread magmatic arcs in the Western Kunlun region provided sources, such as the Kayizi mineralized granodiorite (251 Ma) (Liu et al., 2010), the Taer intrusion granodiorite (227.1 Ma) (Jiang et al., 2013), and the Kangxiwar Xiyeryun plagiogranite (251 Ma) (Yang et al., 2013). Notably, the Permian magmatic rocks discovered by numerous scholars in the West Kunlun region are primarily composed of basic diabase and basalt. Basic igneous rocks typically have low silicon dioxide contents and contain only small numbers of zircons, which are insufficient to serve as the primary zircon source. Therefore, we infer that there may be undiscovered granites, diorites, and other high-silica rocks within the Permian strata of the West Kunlun region. Starting in the Triassic, the subduction of the ancient Tethys Ocean intensified, causing the entire basin to uplift and undergo extensive erosion with minimal deposition. Consequently, no Triassic samples were collected in this experiment. The youngest zircon age identified in this study is 204 $\pm$ 7 Ma, corresponding to the late stages of the evolution of the ancient Tethys Ocean and the final magmatic intrusion events in the West Kunlun region (Jiang et al., 2013; Huang et al., 2013), such as the 204.65 $\pm$ 0.59 Ma Shengliqiao intrusion (Chen et al., 2014).

5.2. Provenance of the West Kunlun piedmont zone

On the basis of the results of the K-S test, it can be seen that the data of our zircon samples are correlated with the data of the four regions, indicating that they may exist source-to-sink relationships. The four regions are the East Kunlun orogenic belt (with a P value of 0.389), the Songpan-Ganzi (with a P value of 0.084), the Tianshuihai terrane (with a P value of 0.031), and the North and South Kunlun terranes (with P values greater than 0.05, such as 0.248). As part of the West Kunlun orogenic belt, the Tianshuihai and the South and North Kunlun terranes are undoubtedly the sources of the piedmont belt. However, whether the East Kunlun orogenic belt and Songpan-Ganzi can confidently be considered the provenance sources of the piedmont belt remains to be determined. The detrital zircons from the Songpan-Ganzi, East Kunlun, Qiangtang, Tianshuihai and North and South Kunlun terranes in the Tethys domain all formed peaks between 260 Ma and 240 Ma, indicating that the beginning of the transition from subduction of the crust of the Paleo-Tethys Ocean to the formation of massive granites by collision orogeny should have occurred within this time range.

The detrital zircon datasets from the Devonian and Jurassic periods are similar (P value of 0.578), and both are strongly correclated with the Devonian strata of the Songpan-Ganzi terrane (P values of 0.084 and 0.301). However, they do not show any association with the Triassic strata. On this basis, it is inferred that during the Devonian, the Songpan-Ganzi terrane was attached to the North and South Kunlun, providing provenance to the Devonian strata of the WKPB. Subsequently, it rifted and returned to the ocean, reattaching to the Tianshuihai, South Kunlun, and North Kunlun terranes during the Jurassic, thereby providing provenance to the Tianshuihai terrane and the piedmont. However, on the basis of the main magmatic intrusion ages (229 Ma-205 Ma) found within the Songpan-Ganzi terrane (Weislogel et al., 2008; Pullen et al., 2008; Deschamps et al., 2017; Chen et al., 2017), there is no evidence of activity during the Devonian. Therefore, classifying the Songpan-Ganzi terrane as a potential provenance area for that period is unreasonable.

According to the K-S test results, East Kunlun is similar primarily between the Jurassic and Cretaceous strata (with P values greater than 0.001, including one P value of 0.389). Previous studies have shown that the East Kunlun orogen began experiencing collisional orogeny by the late Triassic, coinciding with the uplift of the West Kunlun orogen at that time. The distribution of detrital zircons reveals two peaks at 420 Ma and 250 Ma in East Kunlun, similar to those observed in the West Kunlun region. According to previous studies, the Tethyan evolution in East Kunlun is primarily divided into two cycles: 550 Ma-370 Ma and 290

Ma-200 Ma (Feng et al., 2023), which are similar to those in the West Kunlun region. We hypothesize that the similarity in the K-S test results between East Kunlun and the WKPB is due to similar peak ages and tectonic activities. However, the possibility that East Kunlun did indeed provide provenance to the WKPB cannot be ruled out.

5.3. Evolution of the Proto-Tethys in the WKOB

With the breakup of the Rodinia supercontinent, the West Kunlun region developed a complex ocean-continent configuration that was characterized by multiple blocks and ocean basins. The late Neoproterozoic-early Paleozoic is generally considered an important period in the geological evolution of Gondwana, as the initial subduction of the Proto-Tethys Ocean along Gondwana's continental margin occurred during this period (Murphy et al., 2011; Zhu et al., 2012b; Zhao et al., 2018). However, the time limit for subduction in the Proto-Tethys Ocean has been controversial. As an important part of Gondwana, the subduction time for the Proto-Tethys Ocean in the WKOB is also a concern (Liu et al., 2014; Li et al., 2018; Wang et al., 2020). West Kunlun experienced frequent magmatic activity during the early Paleozoic. On the basis of the main timing of magmatic activity in the three terranes of West Kunlun, the subduction of the Proto-Tethys Ocean is likely to have been diachronous. Previous studies have identified 525 Ma syenogranites (Zhang et al., 2004a) and 510 Ma quartz diorites (Xiao et al., 2003) from a rifting environment in the Ku'erti suture zone. Combined with the granite data collected from the South and North Kunlun terranes, which include granites indicative of oceanic crust subduction, and with the oldest granodiorite samples dating to approximately 510 Ma, we infer that the subduction of the Proto-Tethys Ocean beneath the South and North Kunlun terranes occurred after 510 Ma and involved bidirectional subduction. In contrast, previous researchers discovered 533 Ma granites in the Tianshuihai terrane (Liu et al., 2019), indicating that the initial subduction of the Proto-Tethys Ocean likely occurred before 533 Ma. Later, Sui et al., (2023) identified 550.4 Ma granites in the Tianshuihai terrane, which represents the earliest record of Paleozoic magmatic activity in the Tianshuihai region. This suggests that the initial subduction of the Tianshuihai terrane occurred at approximately 550 Ma. Our detrital zircon data show a distinct trough after 600 Ma, reaching the lowest point at approximately 560 Ma. Considering the aforementioned granite evidence, we infer that the initial subduction of the Proto-Tethys Ocean in West Kunlun likely occurred at approximately 560 Ma.

After experiencing the subduction of oceanic crust, no collision-type granites were found within the Tianshuihai terrane or its surrounding terranes, and there was also no detrital zircon peak at approximately 500 Ma in the Tianshuihai terrane itself. We hypothesize that the subduction of the oceanic crust may have temporarily ceased or slowed significantly during this period, which would have been insufficient to generate magmatic activity. There is no specific summary provided by previous studies regarding the timing of the collision, orogeny, post-collision, and the eventual cessation of the Proto-Tethys Ocean subduction. A large distribution of detrital zircons within the same period typically indicates substantial granite generation during that period. Oceanic crust subduction itself usually does not directly produce a significant amount of granite. The large-scale formation of granite is associated primarily with collisional orogenic belts and crustal thickening and partial melting processes that occurred during post-collisional stages. During the Ordovician to Devonian time interval, the detrital zircon ages in our study exhibit a pronounced pattern of peaks and troughs, which is consistent with the detrital zircon age distributions obtained from other terranes within the Tethys domain (see Fig. 6). This pattern is a characteristic hallmark of the tectonic evolution of the Proto-Tethys. On the basis of our analysis of magmatic rock data from the West Kunlun region, the distribution of igneous rocks during this period appears to be continuous. Concurrently, a series of collisional-type magmatic rocks have been identified in the West Kunlun region, such as the 442 Ma biotite granite body in the eastern part of West Kunlun (Han, 2002) and the 421 Ma Subash northern collisional-type monzonite granite (Han, 2006). Combining these observations with the detrital zircon peak at approximately 445 Ma in this study, we infer that the tectonic background of West Kunlun transitioned from oceanic crust subduction to an intracontinental collisional stage before 445 Ma. This is closely aligned with the peak ages of the magmatic rocks in the South Kunlun terrane within this age range. Our detrital zircon ages do not provide a specific closure time for the Proto-Tethys Ocean. However, from a broader regional perspective, Liu, et al., (2012) identified 407 Ma granodiorites and 406 Ma diorites in East Kunlun, suggesting that the terrane collisions in this region were completed by this time and that the region began to enter a rifting phase. Liu, et al., (2013) also discovered 408 Ma diorites in North Qinling, interpreting them as products of the post-collisional period. Considering that the 420 Ma to 405 Ma A-type granites emerging from the reservoir in West Kunlun grew in an intraplate extensional environment and that the detrital zircon dating results indicate that the Proto-Tethys Ocean closure between the South Kunlun terrane and the Tarim landmass occurred from 431 Ma to 420 Ma (Yuan et al., 2002; Xiao et al., 2005; Wang et al., 2020). Comparing these findings with those from other Tethyan domain terranes, the period for the collision of the Proto-Tethys Ocean in the West Kunlun region between 431 Ma and 420 Ma is considered reasonable. The timing of the final closure of the Proto-Tethys Ocean has not been specifically explained by previous studies. During the post-collisional stage, the crust was in a rifting tectonic environment, which could have led to further partial melting of the crust and the formation of late-stage granite intrusions. However, these granites are typically small in scale. From the kernel density plot generated from the ages of the igneous rocks we statistically analysed (Fig. 7), it is evident that the age approaches zero at 380 Ma. Our detrital zircon age distribution reveals a significant trough between 380 Ma and 320 Ma. On the basis of these observation, we infer that by 380 Ma, the evolution of the Proto-Tethys Ocean in the West Kunlun region had completely ceased, and the area entered a brief stable period characterized by minimal magmatic activity. Thus, the entire duration of the Proto-Tethys Ocean, from the onset of oceanic crust subduction to its complete closure, lasted more than 180 Myr (Fig. 7 and Fig. 8).

5.4. Evolution of the Paleo-Tethys in the WKOB

In contrast to the rifting and gradual formation of the Proto-Tethys Ocean, which began before 600 Ma during the rifting of the Rodinia supercontinent, the formation of the Paleo-Tethys Ocean was driven by the development of rift valleys and ocean basin expansion within a regional extensional context. Evidence regarding the temporal overlap between the Proto-Tethys Ocean and the Paleo-Tethys Ocean in the West Kunlun region is also insufficient. Previous studies have confirmed the occurrence of continuous magmatic activity in the South Kunlun region during the Carboniferous period (340 Ma-310 Ma), defining it as a product of rifting and back-arc extension of the Paleo-Tethys Ocean. Thus, at this time, the Paleo-Tethys Ocean may have already opened and begun to subduct beneath the South Kunlun terrane. (Kang et al., 2015; Ji et al., 2018). Combining our detrital zircon data with the collected igneous rock age data, we observe a significant trough between 380 Ma and 340 Ma, with only a single zircon record between 370 Ma and 350 Ma, which indicates that the continuity between the tectonic evolution processes of the Paleo-Tethys Ocean and the Proto-Tethys Ocean is very limited, with a gap of approximately 40 Ma. The Paleo-Tethys Ocean in the West Kunlun region appears to have been inherited from the Proto-Tethys Ocean. The K-S test reveals that from the Permian onwards, the zircons from the South and North Kunlun regions are similar to the detrital zircon dataset from the WKPB (the P value for the Permian is 0.031, whereas the P values for the Cretaceous are all greater than 0.001, with two P values exceeding 0.05), indicating a significant shift in the provenance of the piedmont tectonic belt during the Permian.

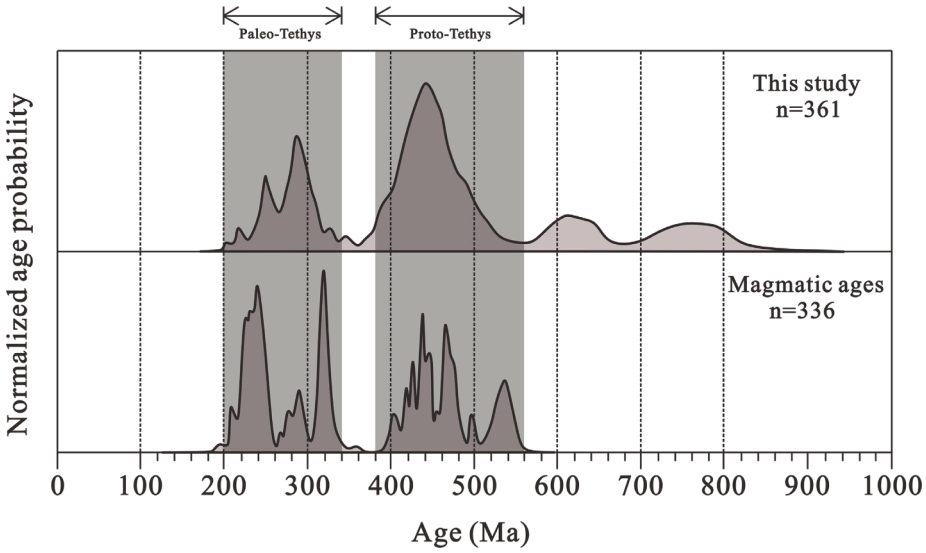

Fig. 7. All detrital zircons younger than 600 Ma and known magmatic zircons.

During the Carboniferous, the West Kunlun region was influenced by the rifting of the Paleo-Tethys Ocean, leading to widespread rift valleys, and the South Kunlun terrane developed back-arc basins. However, during the Permian period, previous studies identified only limited distributions of magmatic rocks within the WKOB, predominantly consisting of intermediate to basic magmatic rocks. These may represent the subduction of oceanic crust and the closure of continental blocks within the arc-backarc basin. This contrasts with the results obtained from our detrital zircon analysis. On the basis of the age distribution of the detrital zircons obtained from the internal and surrounding areas of the research site, a substantial number of detrital zircons dating to approximately 290 Ma have been identified in the Triassic strata of the Tianshuihai area, which are believed to have originated from within the WKOB (Dong et al., 2019). Correspondingly, it is reasonable to assert that the peak formation in the WKPB at 290 Ma aligns with this finding. This suggests that Permian granites, which may be present but undetected in West Kunlun, could correspond to the absence of peaks in the detrital zircon ages from the South and North Kunlun. We infer that Permian granites likely exist in the Tianshuihai terrane (a region that has been less studied by previous researchers) and the Proto-Tethys Ocean subduction in this terrane probably began during the late Carboniferous to early Permian, leading to a series of regional collisional orogenies that provided provenance to the WKPB from the South and North Kunlun terranes.

The timing of the final closure of the Paleo-Tethys Ocean, which signifies the complete transition of the Paleo-Tethys Ocean evolution from oceanic crust subduction to continental collision orogeny, was crucial. The results from the K-S test reveal a significant change in our sample dataset compared with that of the potential source area during the Jurassic. Specifically, the dataset, which was similar to that of the piedmont tectonic belt, shifted from the North and South Kunlun terranes to the Tianshuihai terrane. Considering the youngest single-grain zircon age (204 ± 7 Ma) along with the confirmed sedimentary characteristics of the Cretaceous fluvial facies (Zeng et al., 2020), we preliminarily infer that the Tianshuihai terrane had already accreted by the Jurassic period. Considering the abundant previously reported Triassic collisional granites (Jiang et al., 2013; Zhang et al., 2016; Liu et al., 2015), we establish that the final closure of the Paleo-Tethys Ocean occurred between 243 Ma and 225 Ma. Post-collisional intrusions with ages ranging from 220 Ma to 201 Ma are distributed across regions such as West Kunlun and the Tianshuihai microterrane (Yuan et al., 2002; Liu et al., 2015). The timing of the final cessation of Paleo-Tethys evolution shows good correspondence between the detrital zircon and magmatic rock records, both reaching a minimum value at 190 Ma, after which no further zircon records are found. This corresponded to the end of the post-collisional extensional phase and marked the final extinction of the Paleo-Tethys Ocean. On this basis, we estimate that the duration of the Paleo-Tethys Ocean from its inception to its complete closure was approximately 150 Myr (Fig. 7 and Fig. 8).

6. Conclusions

1. On the basis of a comprehensive analysis of detrital zircon and magmatic zircon data, we propose that the West Kunlun Orogen experienced two distinct evolutionary processes from the original Tethys to the Paleo-Tethys: the Proto-Tethys orogenic cycle from 560 Ma to 380 Ma and the Paleo-Tethys orogenic cycle from 340 Ma to 190 Ma. These two Tethyan cycles are not continuous, with a 40 Ma gap between them.
2. The provenance of the piedmont tectonic belt is primarily located within the West Kunlun orogenic belt. On the basis of the Tethyan orogenic cycles and statistical data analysis, we propose that the evolution of the provenance of the piedmont tectonic belt underwent two distinct changes, which occurred during the Permian and Jurassic periods. In the Permian, due to oceanic crust subduction and regional land-land collisions, West Kunlun transitioned from regional extension to regional uplift, with the South and North Kunlun terranes beginning to supply sediment continuously to the West Kunlun piedmont tectonic belt. During the Triassic, the Tianshuihai terrane completed its collage with the South and North Kunlun terranes, providing provenance to the piedmont tectonic belt over a short period.
3. The peak age of the detrital zircons at approximately 290 Ma contrasts with the currently observed magmatic records in the West Kunlun region. We hypothesize that there may be undiscovered Permian granites within the West Kunlun orogenic belt.

CRediT authorship contribution statement

Yang Gao: Writing – original draft, Methodology, Investigation, Data curation, Conceptualization. **Lin Jiang:** Project administration, Investigation, Funding acquisition. **Weiyan Chen:** Writing – review & editing, Methodology, Conceptualization. **Hongkui Dong:** Supervision, Project administration. **Fujie Jiang:** Supervision, Conceptualization. **Wen Zhao:** Writing – review & editing. **Yingqi Feng:** Investigation. **Liu Cao:** Data curation. **Xuanwei Liu:** Investigation.

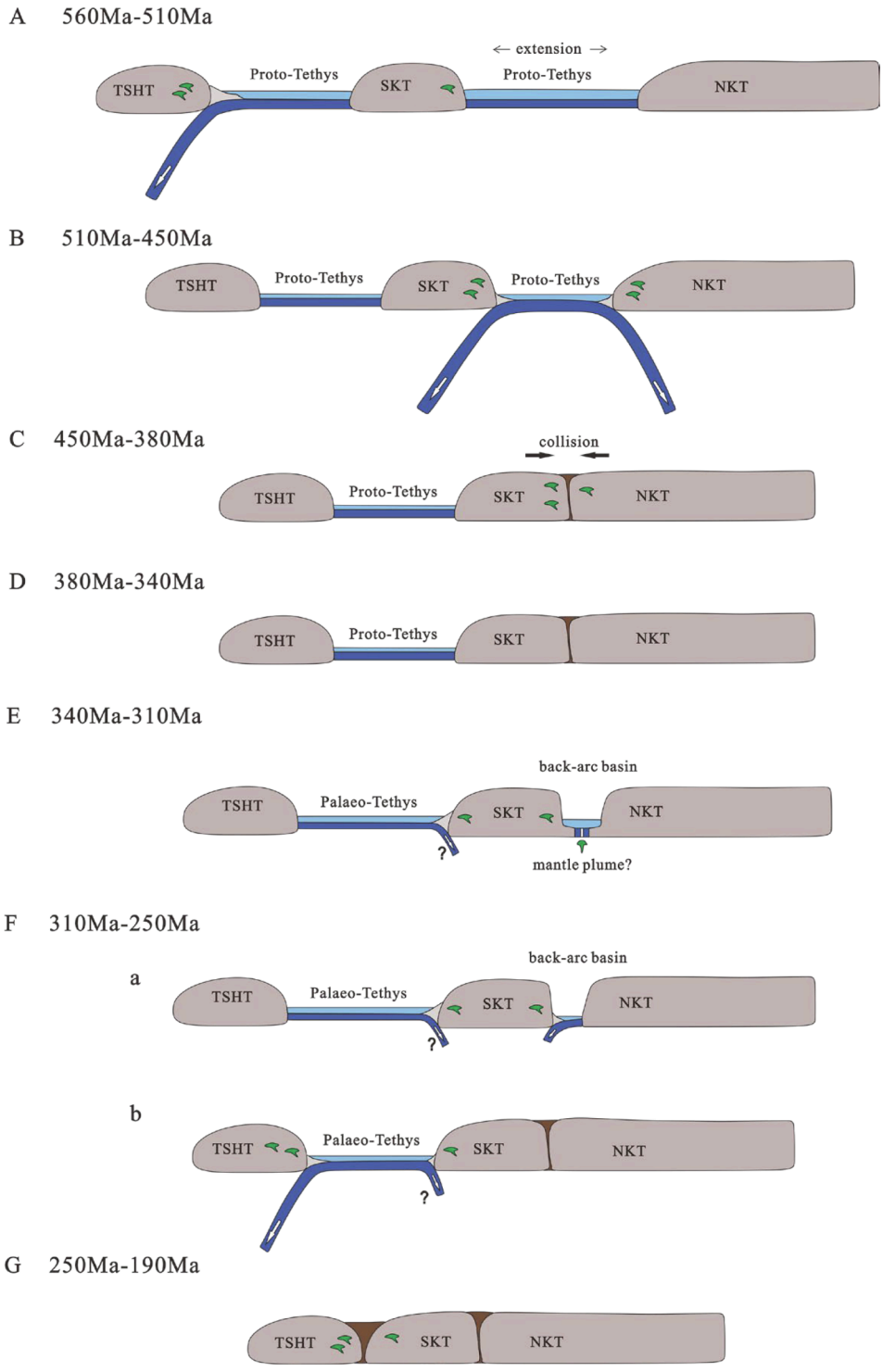

Fig. 8. (A) Initial subduction of the Proto-Tethys Ocean, (B) Bidirectional subduction of the Proto-Tethys Ocean crust between SKT and NKT, (C) Collision between SKT and NKT, marking the end of the Proto-Tethys Ocean evolution, (D)West Kunlun tectonic stability period, (E) Rifting between SKT and NKT generated back-arc basins, (F) a. Subduction of the back-arc ocean crust; b. Subduction of the Paleo-Tethys Ocean crust, (G) The extinction of the Paleo-Tethys Ocean and the eventual formation of the West Kunlun orogenic belt.

Declaration of competing interest

The authors declare that they have no known competing financial interests or personal relationships that could have appeared to influence the work reported in this paper.

Acknowledgments

This work was supported by the Second Tibetan Plateau Scientific Expedition and Research Program (STEP), Grant No. 2019QZKK0708, and the National Natural Science Foundation of China, Grant No. U22B6002.

Appendix A. Supplementary data

Supplementary data to this article can be found online at https://doi.org/10.1016/j.gr.2025.02.010.

References

Allen, M.B., Song, S.G., Wang, C., Zeng, R.Y., Wen, T., 2023. An oblique subduction model for closure of the Proto-Tethys and Palaeo-Tethys oceans and creation of the Central China Orogenic Belt. Earth Sci. Rev. 240, 104385.

Blayney, T., Najman, Y., Dupont-Nivet, G., Carter, A., Millar, I., Garzanti, E., Sobel, R., Rittner, E., Ando, M., Guo, S., Vezzoli, Z.J., 2016. Indentation of the Pamirs with respect to the northern margin of Tibet: Constraints from the Tarim basin sedimentary record. Tectonics. 35 (9–10), 2345–2369.

Cao, K., Wang, G., Bernet, M., van der Beek, P., Zhang, K., 2015. Exhumation history of the West Kunlun Mountains, northwestern Tibet: evidence for a long-lived, rejuvenated orogen. Earth Planet. Sci. Lett. 432, 391–403.

Cawood, P.A., Nemchin, A.A., 2000. Provenance record of a rift basin: U/Pb ages of detrital zircons from the Perth Basin. Western Australia. Sedimentary Geol. 134, 209–234.

Chen, L., Tang, H.W., Ren, Q.J., Zhang, J., Shi J.B., 2014. The Recognition of Shengliqiao Rock Mass of Saliyakedaban,West Kunlun. Northwest. Geol. 47(04). 61-72. in Chinese with English abstract.

Chen, G.M., Liu, J.C., Wang, Y.T., Hu, Q.Q., Huang, S.K., Sun, Z.H., Nijiati, A.B.D.X., Kong, D.Y., Liu, J.F., 2020. Zircon U-Pb Dating and Geochemical Characteristics of Early Paleozoic Granitein the Southern Sunake of West Kunlun,Northwest Chinaand Their Geological Significances. J. Earth Sci. Environ. 2020, 42(4): 427-441. in Chinese with English abstract.

Chen, J.L., Xu, J.F., Ren, J.B., Huang, X.X., 2017. Late Triassic E-MORB-like basalts associated with porphyry Cu-deposits in the southern Yidun continental arc, eastern Tibet: Evidence of slab-tear during subduction? Ore Geol. Rev. 90, 10541062.

Cui, J.T., Wang, J.C., Bian, X.W., Zhu, H.P., Luo, Q.Z., Yang, K.J., Wang, M.C., 2007. Zircon SHRIMP U-Pb dating of Early Paleozoie granite in the Menggubao-Pushou area on the northern side of Kangxiwar,West Kunlun. Geol. Bull. China. 2007, 26(6): 710-719. in Chinese with English abstract.

Deschamps, F., Duchêne, S., de Sigoyer, J., Bosse, V., Benoit, M., Vanderhaeghe, O., 2017. Coeval Mantle-Derived and Crust-Derived Magmas Forming Two Neighbouring Plutons in the Songpan Ganze Accretionary Orogenic Wedge (SW China). J. Petro. 58 (11), 2221–2256.

Dewey, J.F., Horsfield, B., 1970. Plate Tectonics, Orogeny and Continental Growth. Nature. 225, 521–525.

Dewey, J.F., Shackleton, R.M., Chang, C., Sun, Y., 1988. The tectonic evolution of the Tibetan Plateau. Philosophical Transactions of the Royal Society of London A. 327, 379–413.

Ding, L., Yang, D., Cai, F.L., A, Pullen., P, Kapp., G.E, Gehrels., Zhang, L.Y., Zhang, Q.H., Lai, Q.Z., Yue,Y.H., Shi R.D., 2013. Provenance analysis of the Mesozoic Hoh-Xil-SongpanGanzi turbidites in northern Tibet: implications for the tectonic evolution of the eastern Paleo-Tethys Ocean. Tectonics, 32, 34-48.

Dong, Y.P., Sun, S.S., Santosh, M., Zhao, J., Sun, J.P., He, D.F., Shi, X.H., Hui, B., Cheng, C., Zhang, G.W., 2021. Central China Orogenic Belt and amalgamation of East Asian continents. Gondwana Res. 100, 131–194.

Dong, R., Wang, H., Yan, Q.H., Zhang, X.Y., Wei, X.P., Li, P., Zhou, K.L., 2019. Geochemical Characteristics and Zircon U-Pb Ages of the Bayankalashan Group in the Tianshihai Terrain of the West Kunlun Orogenic Belt: Implication for its Provenance and Tectonic Environment. Geotecton. Metallog. 43 (6), 1236–1257 in Chinese with English abstract.

Eizenhöfer, P.R., Zhao, G.C., 2018. Solonker Suture in East Asia and its bearing on the final closure of the eastern segment of the Palaeo-Asian Ocean. Earth Sci. Rev. 186, 153–172.

Eizenhöfer, P.R., Zhao, G.C., Zhang, J., Sun, M., 2014. Final closure of the PaleoAsian Ocean along the Solonker Suture Zone: Constraints from geochronological and geochemical data of Permian volcanic and sedimentary rocks. Tectonics. 33, 441–463.

Eizenhöfer, P.R., Zhao, G.C., Sun, M., Zhang, J., Han, Y.G., Hou, W.Z., 2015. Geochronological and Hf isotopic variability of detrital zircons in Paleozoic strata across the accretionary collision zone between the North China craton and Mongolian arcs and tectonic implications. Geol. Soc. Am. Bull. 127 (9–10), 1422–1436.

Feng, D., Wang, C., Song, S.G., Xiong, L., Zhang, G.B., Allen, Mark.B., Dong, J., Wen, T., Su, L., 2023. Tracing tectonic processes from Proto-to Paleo-Tethys in the East Kunlun Orogen by detrital zircons. Gondwana Res. 115, 1-16.

Gao, X.F., Xiao, P.X., Kang, L., Zhu, H.P., Guo, L., Xi, R.G., Dong, Z.C., 2013. Origin of the volcanic rocks from the Ta' axi region, Taxkorgan Xinjiang and its geological significance. Earth Science. J. China Uni. Geosci. 38, 1769–11182 in Chinese with English abstract.

Ge, R.F., Zhu, W.B., Zheng, B.H., Wu, H.L., He, J.W., Zhu, X.Q., 2012. Early Pan-African magmatism in the Tarim Craton: Insights from zircon U-Pb-Lu-Hf isotope and geochemistry of granitoids in the Korla area. NW China. Precambrian Res. 2012 (212–213), 117–138.

Ge, R.F., Zhu, W.B., Wu, H.L., He, J.W., Zheng, B.H., 2013. Zircon U-Pb ages and Lu-Hf isotopes of Paleoproterozoic metasedimentary rocks in the Korla Complex, NW China: Implications for metamorphic zircon formation and geological evolution of the Tarim Craton. Precambrian Res. 231, 1–18.

Ge, R.F., Wilde, S.A., Zhu, W.B., Zhou, T., Si, Y., et al., 2022. Formation and Evolution of Archean Continental Crust: A Thermodynamic - Geochemical Perspective of Granitoids from the Tarim Craton. NW China. Earth. Sci. Rev. 2022 (234), 104219.

Gehrels, G., Kapp, P., Decelles, P., Pullen, A., Blakey, R., Weislogel, A., Ding, L., Guynn, J., Martin, A., McQuarrie, N., Yin, A., 2011. Detrital zircon geochronology of pre-Tertiary strata in the Tibetan-Himalayan orogen. Tectonics. 30 (5), TC5016.1-TC5016.27.

Guo, X.C., Zheng, Y.Z., Gao, J., Zhu, Z.X., 2013. Determination and Geological Significance of the Mesoarchean Craton in Western Kunlun Mountains , Xinjiang , China. Geol. Rev. 59(03), 401-412. in Chinese with English abstract.

Han, F.L., 2002. Qimanyuter Ophiolite Melange And Its Tectonic Significance,Western Kunlun Mountain,NW China. China University of Geosciences (Beijing). in Chinese with English abstract.

Han, F.L., 2006. Tectonic evolution and mineralizationof the western Kunlun accretion-type orogen. China University of Geosciences (Beijing). in Chinese with English abstract.

Hu, N., 2014. Geologic Features,Provenance Analysis and Structural Evolution of Maerzheng Formation at the Buqingshan Area in the Southern Margin of the East Kunlun region. Changan University. in Chinese with English abstract.

Hu, J., Wang, H., Huang, C.Y., Tong, L.X., Mu, S.L., Qiu, Z.W., 2016. Geological characteristics and age of the Dahongliutan Fe-ore deposit in the Western Kunlun orogenic belt, Xinjiang, northwestern China. J. Asian Earth Sci. 116, 1–25.

Huang, X.H., 2016. Provenance and Tectonic Implications of the Gequ Formation at Area North of Huashixia. China University of Geosciences. in Chinese with English abstract, East Kunlun Region.

Huang, J.G., Yang, R.D., Yang J., Cui, C.L., 2013. Geochemical characteristics and tectonic significance of Triassic Granite from Taer Region, the Northern Margin of West Kunlun. Acta Geol. Sinca (English Edition). 2013, 87(2), 346-357.

Huang, F., Xu, J.F., Wang, B.D., Zeng, Y.C., Liu, X.J., Liu, H., Yu, H.X., 2020. Destiny of Neo-Tethyan Lithosphere during India-Asia Collision. Earth Sci. 45(08): 2785-2804. in Chinese with English abstract.

Ji, W.H., Chen, S.J., Li, R.S., He, S.P., Zhao, Z.M., Pan, X.P., 2018. The origin of Carboniferous-Permian magmatic rocks in Oytag area,West Kunlun:Back-are basin? Acta Petro. Sinica. 34(8), 2393-2409. in Chinese with English abstract.

Jia, R.Y., Jiang, Y.H., Liu, Z., Zhao, P., Zhou, Q., 2013. Petrogenesis and tectonic implications of early Silurian high-K calc-alkaline granites and their potassic microgranular enclaves, western Kunlun orogen, NW Tibetan Plateau: Int. Geol. Rev. 55, 958–975.

Jiang, L., Dong, H.K., Li, Y., Zhao, W., Zhang, Y.Q., Bo, D.M., 2024. Deformation characteristics and exploration potential of the West Kunlun fold-and-thrust belt. Adv. Geo-Energy Res. 11 (3), 181–193.

Jiang, Y.H., Jiang, S.Y., Ling, H.F., Zhou, X.R., Rui, X.J., Yang, W.Z., 2002. Petrology and geochemistry of shoshonitic plutons from the West Kunlun orogenic belt, northwestern Xinjiang, China: implications for granitoid geneses. Lithos. 63, 165–187.

Jiang, Y.H., Jia, R.Y., Liu, Z., Liao, S.Y., Zhao, P., Zhou, Q., 2013. Origin of Middle Triassic high-K calc-alkaline granitoids and their potassic microgranular enclaves from the West Kunlun orogen, northwest China: a record of the closure of Paleo-Tethys. Lithos. 156–159, 13–30.

Kang, L., Xiao, P.X., Gao, X.F., Wang, C., Yang, Z.C., Xi, R.G., 2015. Geochemical characteristics,petrogenesis and tectonic seting of Oceanic plagiogranites belt in the northwestern margin of western Kunlun. Acta Petro. Sinica. 31 (9), 2566–2582 in Chinese with English abstract.

Kendall, B., Creaser, R.A., Selby, D., 2006. Re-Os geochronology of postglacial black shales in Australia: Constraints on the timing of Sturtian glaciation. Geology. 34 (9), 729–732.

Li, D., Han, Y.G., Zhao, G.C., Zhou, M.F., He, D.F., Hou, S.Q., Zhen, Y., Fan, D., Yang, H., 2024. Sedimentary provenance supports a mid-paleozoic tectonic connection between the Junggar and Altai terranes in central Asia. Sci Rep. 14, 22502 (2024).

Li, B.Q., Yao, J.X., Ji, W.H., Zhang, J.L., Yin, Z.Y., Chen, G.C., Lin, X.W., Zhang, Q.S., Kong, W.N., Wang, F., Liu, X.P., 2006. Characteristics and ziron SHRIMP U-Pb ages of the arc magmatic rocks in Mazar, southern Yecheng. West Kunlun Mountains. Geol. Bull. China. 25 (1–2), 124–132 in Chinese with English abstract.

Li, S.Z., Zhao, S.J., Yu, S., Cao, H.H., Li, X.Y., Liu, X., Guo, X.Y., Xiao, W.J., Lai, S.C., Yan, Z., Li, Z.H., Yu, S.Y., Zhang, J., Lan, H.Y., 2016. Proto-Tehtys Ocean in East Asia (II): Affinity and assmbly of Early Paleozoic micro-continental blocks. Acta Petro. Sinica. 32 (9), 2628–2644 in Chinese with English abstract.

Li, S.Z., Zhao, S.J., Liu, X., Cao, H.H., Yu, S., Li, X.Y., Somerville, I., Yu, S.Y., Suo, Y.H., 2018. Closure of the Proto-Tethys Ocean and Early Paleozoic amalgamation of microcontinental blocks in East Asia. Earth.sci. Rev. 186, 37–75.

Liu, F., 2006. Songpan-Ganzi block and the Longmen mountainsClastic sedimentary rocks geochemistry. China University of Geosciences (Beijing). In Chinese with English Abstract.

Liu, C.J., 2013. Study on Material Composition, Tectonic Evolution and Transformation at the Conjunction of Qinling and North Qilian Orogen. Changan University. In Chinese with English Abstract.

Liu, C.J., 2015. Composition and Tectonic Evolution of West Kunlun Orogenic Belt and its Periphery in the Early Paleozoic-Early Mesozoic. Changan University. In Chinese with English Abstract.

Liu, Z., Jiang Y H., Jia R Y., Zhao, P., Zhou, Q., Wang, G.C., Ni, C.Y., 2014. Origin of Middle Cambrian and Late Silurian potassic granitoids from the western Kunlun orogen,northwest China: a magmatic response to the Proto-Tethys evolution. Mineral. Petro. 2014, 108(1), 91-110.

Liu, X.Q., Zhang, C.L., Ye, X.T., Zou, H.B., Hao, X.S., 2019. Cambrian mafic and granitic intrusions in the MazarTianshuihai terrane, West Kunlun Orogenic Belt: Constraints on the subduction orientation of the Proto-Tethys Ocean. Lithos, 350.

Liu, Z., Jiang, Y.H., Jia, R.Y., Zhao, P., Zhou, Q., 2015. Origin of Late Triassic high-K calc-alkaline granitoids and their potassic microgranular enclaves from the western Tibet Plateau, northwest China: Implications for Paleo-Tethys evolution. Gondwana Res. 27, 326–341.
Liu, B., Ma, C.Q., Zhang, J.Y., Xiong, F.H., Huang, J., Jiang, H.A., 2012. Petrogenesis ofEarly Devonian intrusive rocks in the east part of Eastern Kunlun Orogen and implication for Early Palaeozoic orogenic processes. Acta Petro. Sinica. 28 (6), 1785–1807 in Chinese with English abstract.
Liu, J.P., Wang, H., Li, S.H., Tong, L.X., Ren, G.L., 2010. Geological and geochemical features and geochronology of the Kayizi porphyry molybdenum deposit in the northern belt of western Kunun NW China. Acta Petro. Sinica 26 (10), 3095–3105 in Chinese with English abstract.
Liu, C.H., Zhao, G.C., Liu, F.L., Shi, J.R., 2017. Detrital zircon U-Pb and Hf isotopic and whole-rock geochemical study of the Bayan Obo Group, northern margin of the North China Craton: Implications for Rodinia reconstruction. Precambrian Res. 303, 372–1291.
Liu, Q., Zhao, G.C., Han, Y.G., Zhu, Y.L., Wang, B., Eizenhöfer, P.R., Zhang, X.R., 2019a. Detrital zircon provenance constraints on the final closure of the middle segment of the Paleo-Asian Ocean. Gondwana Res. 69, 73–88.
Lu, Q.Y., 2022. Mesozoic tectonic process in southwestern Tarim Basin and its constraints on the dynamic evolution of the Paleo-Tethys orogenic belt. Zhejiang University. In Chinese with English Abstract.
Lu, S.N., Li, H.K., Zhang, C.L., Niu, G.H., 2008. Geological and geochronological evidence for the Precambrian evolution of the Tarim Craton and surrounding continental fragments. Precambrian Res. 160 (1–2), 94–107.
Mahar, M.A., Mahéo, G., Goodell, P.C., Pavlis, T.L., 2014. Age and origin of post collision Baltoro granites, south Karakoram, North Pakistan: insights from insitu UePb, Hf and oxygen isotopic record of zircons. Lithos. 205, 341–358.
Matte, P., Tapponnier, P., Arnaud, N., Bourjot, L., Avouac, J.P., Vidal, P., Liu, Q., Pan, Y., Wang, Y., 1996. Tectonics of western Tibet,between the Tarim and the Indus. Earth Planet. Sci. Lett. 142, 311–330.
Mattern, F., Schneider, W., Li, Y., 1996. A traverse through the western Kunlun (Xinjiang, China): tentative geodynamic implications for the Palaeozoic and Mesozoic. Geol, Rundschau, p. 85.
Mattern, F., Schneider, W., 2000. Suturing of the Proto- and Paleo-Tethys oceans in the West Kunlun (Xijiang, China). J.asian Earth Sci. 18, 637–650.
Meert, J., 2003. A synopsis of events related to the assembly of eastern Gondwana. Tectonophysics. 362, 1–40.
Metcalfe, I., 2009. Late Palaeozoic and Mesozoic tectonic and palaeogeographical evolution of SE Asia. Gondwana Res. 315, 7–23.
Mo, X.X., Pan, G.T., 2006. From the Tethys to the formation of the Qinghai-Tibet Plateau: constrained by tectono-magmatic events. Earth Sci Front. 13 (6), 043–051.
Murphy, J.B, Van, Staal.C.R, Collins, W.J., 2011. A comparison of the evolution of arc complexes in Paleozoic interior and peripheral orogens: Speculations on geodynamic correlations. Gondwana Res. 19, 812-827.
Pan, Y., Bian, Q., 1996. Geological Evolution of the Karakorum and Kunlun Shan: Beijing. Seismological Press, Tectonics. China, pp. 230-262.
Pan, Y.S., Wang, Y., 1994. Discovery and evidence of the fifth Suture Zone of QinghaieTibetan Plateau. Acta Geoph. Sinica 37, 241-250. in Chinese with English abstract.
Park, J.K., Buchan, K.L., Harlan, S.S., 1995. A proposed giant radiating dyke swarm fragmented by the separation of Laurentia and Australia based on paleomagnetism of ca. 780 Ma mafic intrusions in western North America. Earth Planet. Sci. Lett. 132, 129–139.
Paulsen, T.S., Deering, C., Sliwinski, J., Bachmann, O., Guillong, M., 2016. Detrital zircon ages from the Ross Supergroup, north Victoria Land, Antarctica: implications for the tectonostratigraphic evolution of the Pacific-Gondwana margin. Gondwana Res. 35, 79–96.
Peng, Y.B., Yu, S.Y., Li, S.Z., Zhang, J.X., Liu, Y.J., Li, Y.S., Santosh, M., 2019. Early Neoproterozoic magmatic imprints in the Altun-Qilian-Kunlun region of the Qinghai-Tibet Plateau: Response to the assembly and breakup of Rodinia supercontinent. Earth Sci. Rev. 199, 102954.
Pullen, A., Kapp, P., Gehrels, G.E., Vervoort, J.D., Ding, L., 2008. Triassic continental subduction in central Tibet and Mediterranean-style closure of the Paleo-Tethys Ocean. Geology. 36 (5), 351–354.
Qiao, G.B., Wang, P., Wu, Y.Z., Hao, Y.H., Zhao, X.J., Chen, D.H., Lv, P.R., Du, W., 2015. Formation age of ore-bearing strata of the Zankan irondeposit in Taxkorgan landmass of Western Kunlun Mountains and its geological significance. Geol. China 42, 616–630 in Chinese with English abstract.
Reymond, B.A., Stampfli, G.M., 1996. Three-dimensional sequence stratigraphy and subtle stratigraphic traps associated with systems tracts: West Cameron region, offshore Lousiana, Gulf of Mexico. Marine and Petrol. Geol. 13, 41–60.
Rojas-Agramonte, Y., Kröner, A., Demoux, A., Xia, X., Wang, W., Donskaya, T., Liu, D., Sun, M., 2011. Detrital and xenocrystic zircon ages from Neoproterozoic to Paleozoic arc terranes of Mongolia: Significance for the origin of crustal fragments in the Central Asian Orogenic Belt. Gondwana Res. 19, 751–763.
Santosh, M., Sajeev, K., Li, J.H., 2006. Extreme crustal metamorphism during Columbia supercontinent assembly: Evidence from North China Craton. Gondwana Res. 10 (3–4), 256–266.
Shu, L.S., Deng, X.L., Zhu, W.B., Ma, D.S., Xiao, W.J., 2011. Precambrian Tectonic Evolution of the Tarim Block, Nw China: New Geochronological Insights from the Quruqtagh Domain. J. Asian Earth Sci. 42 (5), 774–790.
Song, S.G., Su, L., Li, X.H., Zhang, G.B., Niu, Y.L., Zhang, L.F., 2010. Tracing the 850-Ma continental flood basalts from a piece of subducted continental crust in the North Qaidam UHPM belt, NW China. Precambrian Res. 183.
Sui, Q.L., 2021. Genesis of magmatic rocks in Western Kunlun Orogenic Belt and implications on the evolution of Proto-Palaeo Tethys Ocean. University of Chinese Academy of Sciences. In Chinese with English Abstract.
Sui, Q.L., Chen, D.H., Zhao, X.J., Zha, X.F., Sun, J.M., Zhang, L.P., Gao, X.F., Sun, W.D., 2023. Diachronous subduction of the Proto-Tethys Ocean along the northern margin of East Gondwana: Insights from SHRIMP and LA-ICP-MS zircon geochronology in the West Kunlun Orogenic Belt. Northwestern China. Inter. Geol. Rev. 65 (7), 1179–1202.
Torsvik, T.H., Eide, E.A., Meert, J.G., Smethurst, M.A., Walderhaug, H.J., 1998. The Oslo Rift: New palaeomagnetic and $^{40}Ar/^{39}Ar$ age constraints. Geoph. J. Inter. 135, 1045–1059.
Turner, C.C., Meert, J.G., Pandit, M.K., Kamenov, G.D., 2014. A detrital zircon U–Pb and Hf isotopic transect across the Son Valley sector of the Vindhyan Basin, India: implications for basin evolution and paleogeography. Gondwana Res. 26, 348–364.
Wan, B., Wu, F.Y., Chen, L., Zhao, L., Liang, X.F., Xiao, W.J., Zhu, R.X., 2019. Cyclical one-way continental rupture-drift in the Tethyan evolution: Subductiondriven plate tectonics. Sci China Earth Sci. 62, 2005–2016.
Wang, Z.H., 2004. Tectonic evolution of the West Kunlun orogenic belt, western China. J. Asian Earth Sci. 24, 153–161.
Wang, P., Zhao, G.C., Han, Y.G., Liu, Q., Yao, J.L., Yu, S., Li, J.H., 2020. Timing of the final closure of the Proto-Tethys Ocean: Constraints from provenance of early Paleozoic sedimentary rocks in West Kunlun. NW China. Gondwana Res. 84, 151–162.
Wei, X.P., 2018. Spatial-temporal Pattern, Petrogenesis and Tectonic Implications of the Triassic Granitoids from the Western Kunlun Orogen, Northwestern China. University of Chinese Academy of Sciences. In Chinese with English Abstract.
Weislogel, A.L., 2008. Tectonostratigraphic and geochronologic constraints on evolution of the northeast Paleotethys from the Songpan-Ganzi complex, central China. Tectonophysics. 451 (1–4), 331–345.
Wu, F.Y., Wan, B., Zhao, L., Xiao, W.J., Zhu, R.X., 2020. Tethyan geodynamics. Acta. petrol. Sinica. 36, 1627–1674 in Chinese with English abstract.
Xiao, W.J., 2023. Plate divergent-convergent coupling system and dynamic mechanism of continental orogenic belts. Sci China Earth Sci. 66 (8), 1909–1912.
Xiao, X.C., Wang, J., Su, L., Song S.G., 2003. A further discussion of the Küda ophiolite, West Kunlun,and its tectonic significance. Geol. Bull. China, 22(10), 745-750. in Chinese with English abstract.
Xiao, W.J., Hou, Q.L., Li, J.L., 1999. Tectonic facies and the archipelagoaccretion process of the West Kunlun, China. Sci. China Earth Sci. 43, 135-143 (suppl.).
Xiao, W.J., Han, F.L., Windley, B.F., Yuan, C., Zhou, H., Li, J.L., 2003a. Multiple accretionary orogenesis and episodic growth of continents: Insights from the Western Kunlun Range, central Asia. Inter. Geol. Rev. 45, 303–328.
Xiao, W.J., Windley, B.F., Liu, D.Y., Jian, P., Liu, C.Z., Yuan, C., Sun, M., 2005. Accretionary tectonics of the Western Kunlun Orogen, China: A Paleozoic-early Mesozoic, long-lived active continental margin with implications for the growth of southern Eurasia. J. Geol. 113, 687–705.
Xiong, L., Song, S.G., Su, L., Zhang, G.B., Allen, M.B., Feng, D., Yang, S.W., 2023. Detrital zircons from high-pressure trench sediments (Qilian Orogen): Constraints on continental-arc accretion, subduction initiation and polarity of the Proto-Tethys Ocean. Gondwana Res. 113, 194–209.
Xu, X., Song, S.G., Su, L., 2016. Formation age and tectonic significance of the Wanbaogou basalts in the middle East Kunlun orogenic belt. Acta Petrol. Mineral. 35, 965-980. in Chinese with English abstract.
Xu, R.H., Zhang, Y.Q., Xie, Y.W., Chen, F.K., Vadal, P., Nicolas, A., Zhang, Q.D., Zhao, D. M., 1994. A discovery of an early Palaeozoic tectonomagmatic belt in the northern part of west Kunlun mountains. Sci. Geol. Sinica. 4, 313–328 in Chinese with English abstract.
Yang, W.Q., 2013. The Indosinian metamorphism, magmatism and formation age of Bunlunkuole rock group in Taxkorgan-Kangxiwar tectonic belt. Northwestern University. in Chinese with English abstract, Western Kunlun.
Yang, W.Q., Liu, L., Cao, Y.T., Wang, C., He, S.P., Li, R.S., Zhu, X.H., 2010. Geochronological evidence of Indosinian (high-pressure) metamorphic event and its tectonic significance in Taxkorgan area of the Western Kunlun Mountains, NW China. Sci China Earth Sci. 2010, 53(10): 1445-1459.
Yang, W., Fu, L., Wu, C., Song, Y., Jiang, Z., Luo, Q., Zhang, Z., Zhang, C., Zhu, B., 2018. U-Pb ages of detrital zircon from Cenozoic sediments in the southwestern Tarim Basin, NW China: Implications for Eocene–Pliocene source-to-sink relations and new insights into Cretaceous–Paleogene magmatic sources. J. Asian Earth Sci. 156, 26–40.
Yang, S.F., Li, Z.L., Chen, H.L., Santosh, M., Dong, C.W., Yu, X., 2007. Permian bimodal dyke of Tarim Basin, NW China: Geochemical characteristics and tectonic implications. Gondwana Res. 12, 113–120.
Ye, X.T., Zhang, C.L., Santosh, M., Zhang, J., Fan, X.K., Zhang, J.J., 2016. Growth and evolution of Precambrian continental crust in the southwestern Tarim terrane: new evidence from the ca. 1.4 Ga A-type granites and Paleoproterozoic intrusive complexg. Precambrian Res. 275, 18–34.
Yi, Z.Y., Wei, G.Q., Guo, Z.J., 2023. Did Grenvillian Orogeny ever Happen in Tarim Craton? Evidence from Detrital Zircon Chronology. Earth Sci. 48 (04), 1405–1420 in Chinese with English abstract.
Yin, A., Harrison, T.M., 2000. Geologic Evolution of the Himalayan-Tibetan Orogen. Ann. Rev. Earth Planet. Sci. 28, 211–280.
Yin, J.Y., Xiao, W.J., Sun, M., Chen, W., Yuan, C., Zhang, Y.Y., Wang, T., Du, Q.Y., Wang, X.S., Xia, X.P., 2020. Petrogenesis of Early Cambrian granitoids in the western Kunlun orogenic belt, Northwest Tibet: Insight into early stage subduction of the Proto-Tethys Ocean. Geol. Soc. Amer. Bull. 132 (9–10), 2221–2240.

Yuan, C., Sun, M., Zhou, M.F., Zhou, H., Xiao, W.J., Li, J.L., 2002. Tectonic evolution of the West Kunlun: geochronologic and geochemical constraints from Kudi granitoids. Inter. Geol. Rev. 44, 653–669.

Zeng, Q.L., Zhang, R.H., Zhang, L., Liu, C., Chen, C., Xia, J.F., 2020. Sedimentary facies and reservoir evolution divergence of Early Cretaceous sandstones in Southwest Depression of Tarim Basin. Natural Gas Geoscience. 2020, 31(10): 1375-1388. in Chinese with English abstract.

Zeng, Q.G., Wang, B.D., Xi, L.L.J., M, Z.G., Liu, H.Y., Liu, G.X., 2020. Suture Zones in Tibetan and Tethys Evolution. Earth Sci. 45(08): 2735-2763. in Chinese with English abstract.

Zhang, Y.Q., Xie, Y.W., Xu, R.H., Vidal, P., Nicolas, A., 1996. Geologic Evolution of the Karakorum and Kunlun Mountains. In: Pan, Y.S. (Ed.). Seismological Press,Beijing, pp. 94-136 (in Chinese).

Zhang, C.L., Yu, H.F., Wang, A.G., Guo, K.Y., 2005. Dating of Triassic Granites in the Western Kunlun Mountains and Its Tectonic Significance. Acta Geologica Sinica. 05, 645-652. in Chinese with English abstract.

Zhang, C.L., Li, Z.X., Li, X.H., Ye, H.M., 2007a. Early Palaeoproterozoic high-K intrusive complex in southwestern Tarim Block, NW China: age, geochemistry and implications for the Paleoproterozoic tectonic evolution of Tarim. Gondwana Res. 12, 101–112.

Zhang, L., Long, X.P., Zhang, R., Dong, Y.P., Yuan, C., Xiao, W.J., Wang, Y.J., 2017. Source characteristics and provenance of metasedimentaryrocks from the Kangxiwa Group in the Western Kunlun Orogenic Belt,NW China: Implications for tectonic setting and crustal growth. Gondwana Res. 46, 43–56.

Zhang, C.L., Yu, H.F., Shen, J.-L., Dong, Y.G., Ye, H.M., Guo, K.Y., 2004. Zircon SHRIMP Age Determination of the Giant-crystal Gabbro and Basaltin K·da,West Kunlun: Dismembering of the K·da Ophiolite. Geol. Rev. 50 (6), 639–643 in Chinese with English abstract.

Zhang, C.L., Lu, S.N., Yu, H.F., Ye, H.M., 2007b. Tectonic evolution of the West Kunlun orogenic belt on the northern margin of the Tibetan Plateau: zircons Evidence for SHRIMP and LA-ICP-MS dating. Sci. China Earth Sci. 2007 (02), 145–154.

Zhang, C.L., Li, H.K., Santosh, M., Li, Z.X., Zou, H.B., Wang, H.Y., Ye, H.M., 2012. Precambrian Evolution and Cratonization of the Tarim Block, NW China: Petrology, Geochemistry, Nd-isotopes and U-Pb Zircon Geochronology from Archaean Gabbro-TTG-Potassic Granite Suite and Paleoproterozoic Metamorphic Belt. J.asian Earth Sci. 47, 5–20.

Zhang, Y., Niu, Y., Hu, Y., Liu, J.J., Ye, L., Kong, J.J., Duan, M., 2016. The syncollisional granitoid magmatism and continental crust growth in the West Kunlun Orogen, China – Evidence from geochronology and geochemistry of the Arkarz pluton. Lithos 245, 191–204.

Zhang, Z.C., Xiao, X.C., Wang, J., Wang, Y., Timothy, M.K., 2008. Post-collisional Plio-Pleistocene shoshonitic volcanism in the western Kunlun Mountains, NW China: Geochemical constraints on mantle source characteristics and petrogenesis. J. Asian Earth Sci. 31, 379–403.

Zhang, C.L., Zou, H.B., Santosh, M., Ye, X.T., Li, H.K., 2014. Is the Precambrian basement of the Tarim Craton in NW China composed of discrete terranes? Precambrian Res. 254, 226–244.

Zhang, C.L., Ye, X.T., Zou, H.B., Chen, X.Y., 2016a. Neoproterozoic sedimentary basin evolution in southwestern Tarim, NW China: New evidence from field observations, detrital zircon U–Pb ages and Hf isotope compositions. Precambrian Res. 280, 31–45.

Zhang, J.X., Yu, S.Y., Li, Y.S., Yu, X.X., Lin, Y.H., Mao, X.H., 2015. Subduction, accretion and closure of Proto-Tethyan Ocean: Early Paleozoic accretion /collision orogeny in the Altun-Qilian-North Qaidam orogenic system. Acta Petrol. Sinica 31 (12), 3531–3554 in Chinese with English abstract.

Zhang, Y.X., Zheng, B., Dai, J., Rosenbaum, G., Wang, J., 2024. Tectonic evolution of the Qiangtang Basin (northern Tibet): Constraints from detrital zircon geochronology. Gondwana Res. 136, 202–218.

Zhang, C.L., Zou, H.B., Ye, X.T., Chen, X.Y., 2018a. Tectonic evolution of the NE section of the Pamir Plateau:New evidence from field observations and zircon U-Pb geochronology. Tectonophysics. 723, 27–40.

Zhang, C.L., Zou, H.B., Ye, X.T., Chen, X.Y., 2018b. Timing of subduction initiation in the Proto-Tethys Ocean: Evidence from the Cambrian gabbros from the NE Pamir Plateau. Lithos. 314–315, 40–51.

Zhang, C.L., Zou, H.B., Ye, X.T., Chen, X.Y., 2019. Tectonic evolution of the West Kunlun Orogenic Belt along the northern margin of the Tibetan Plateau: Implications for the assembly of the Tarim terrane to Gondwana. Geosci. Front. 10 (3), 973–988.

Zhao, G.C., Cawood, P.A., Wilde, S.A., Sun, M., 2002. Review of global 2.1–1.8 Ga orogens: implications for a pre-Rodinia supercontinent. Earth. Sci. Rev. 59 (1–4), 125–162.

Zhao, G.C., Wang, Y.J., Huang, B.C., Dong, Y. P., Li, S.Z., Zhang, G,.W., Yu, S., 2018. Geological reconstructions of the East Asian blocks: From the breakup of Rodinia to the assembly of Pangea. Earth. Sci. Rev. 186, 262-286.

Zhou, T., Ge, R.F., Zhu, W.B., Wu, H.L., 2021. Is There a Grenvillian Orogen in the Southwestern Tarim Craton? Precambrian Res. 354, 106053.

Zhu, R.X., Zhao, P., Zhao, L., 2022. Tectonic evolution and geodynamics of the Neo-Tethys Ocean. Sci. China Earth Sci. 65(1): 1-24. in Chinese with English abstract.

Zhu, J., Li, Q.G., Wang, Z.Q., Tang, H.S., Chen, X., Xiao, B., 2016. Magmatism and tectonic implication of Early Cambrian granitoid plutons in Tianshuhai Terrane of the Western Kunlun Orogenic Belt. Northwest China: Northwest. Geol. 49, 1–18 in Chinese with English abstract.

Zhu, G.Y., Liu, W., Wu, G.H., Ma, B.S., Nance, R.D.M., Wang, Z.C., Xiao, Y., Chen, Z.Y., 2021. Geochemistry and U-Pb-Hf detrital zircon geochronology of metamorphic rocks in terranes of the West Kunlun Orogen: Protracted subduction in the northernmost Proto-Tethys Ocean. Precambrian Res. 363, 106344.

Zhu, D.C., Zhao, Z.D., Niu, Y., Dilek, Y., Wang, Q., Ji, W.H., Dong, G.C., Sui, Q.L., Liu, Y. S., Yuan, H.L., Mo, X.X., 2012. Cambrian bimodal volcanism in the Lhasa Terrane, southern Tibet: Record of an early Paleozoic Andean-type magmatic arc in the Australian protoTethyan margin. Chem. Geol. 328, 290–1230.